Korean J. Chem. Eng., 39(1), 38-57 (2022)
DOI: 10.1007/s11814-021-0941-y

pISSN: 0256-1115
eISSN: 1975-7220

REVIEW PAPER

Biocolloid transport and deposition in porous media: A review

Hongjuan Bai*, Junhang Chen*,†, Yumu Hu*, Gang Wang*,†, Wenju Liu*,†, and Edvina Lamy**

*School of Chemistry and Chemical Engineering, Henan University of Technology, Zhengzhou 450001, P. R. China
**Sorbonne universités, Université de Technologie de Compiègne, UTC/ESCOM, EA 4297 TIMR,
Centre de recherche Royallieu - CS 60 319 - 60 203 Compiègne Cedex, France
(*Received 17 April 2021 • Revised 13 August 2021 • Accepted 26 August 2021*)

Abstract−In an effort to protect surface and groundwater supplies from contamination, to assess the risk of microbial groundwater contamination and for the purpose of soil bioremediation, considerable efforts have been made to investigate biocolloid transport and retention in porous media. The current work provides an introductory overview of biocolloid transport and deposition in porous media so as to have a better understanding of the environmental behavior of biocolloids. In this review, biocolloid transport and deposition in porous media are discussed with an emphasis on transport and deposition mechanisms, numerical modeling and influencing factors. Moreover, major findings with respect to the forces acting on biocolloid transport and deposition are addressed, and research methods used to study biocolloid transport and deposition in porous media are also presented. Finally, based on the reported results, future research perspectives considering the microscopic pore scale study for biocolloid transport and deposition in porous media are also suggested.

Keywords: Biocolloid, Particle Transport, Porous Media, Retention

INTRODUCTION

In subsurface environments, various inorganic and organic materials, such as mineral precipitates, rock and mineral fragments, weathering products and macromolecular components of dissolved organic carbon) exist as colloids [1]. Colloids are often defined as particles with characteristic diameters ranging from 1 nm to 10 μm [2]. Considering the size, microbial pathogens such as bacteria, viruses, spores and protists are referred to as biocolloids [3]. Generally, the sizes of biocolloid range from about 200 nm to 5 μm, which correspond to the pore size of coarse clay to fine silt (Fig. S1). Therefore, biocolloid can easily move through porous media in the subsurface environment. Based on the air and water content in soil subsurface, three zones are commonly divided as follows: (i) The zone from the ground surface to an aquifer water table refers to "water unsaturated zone or vadose zone". In this zone, pore spaces are mostly occupied by the air with some adsorbed and capillary-held water contained in soils; (ii) The zone from the top of water table to bedrock refers to the "saturated zone", which contains mostly water in the pore spaces; (iii) The transition region between the vadose and saturated zones refers to the "capillary zone".

Most of the biocolloids released to the subsurface environment originate from human and animal sewage from nearby municipal wastewater discharges, septic tanks, sanitary landfills and agricultural practices [4]. These can travel through the vadose zone further down the subsurface. The presence of these biocolloids in drinking water can result in the serious outbreaks of waterborne disease [5-8]. One such tragic event occurred in May 2000 in Walkerton, when bacterial contamination of drinking water resulted in medical attention required by 2300 people, 7 of whom died [9]. The tragic incident happened despite the city following best management practices for waste disposal. Many researchers have investigated this event and reported that biocolloids released into the soil through sewage irrigation and tank effluent travelled rather long distances in soils, especially following heavy rainfall [10]. Thus, it is very critical to understand biocolloid transport patterns, which has great practical importance with respect to the planning, design and management of biological wastewater treatment units. Moreover, a better understanding of the mechanisms governing biocolloid transport and retention in porous media is necessary for a wide variety of applications, including water treatment [11,12], microbially enhanced oil recovery [13], bioremediation and bioaugmentation [14-16], and assessing and mitigating the risk of pathogen contamination [15-17].

Considerable amounts of research have been directed to this topic [18-25], and several good review articles focusing on specific topics of different processes or behaviors of biocolloids in porous media and the environment have been published [26-34]. The objective of this work was to be an introductory overview on the relevant research concerning biocolloid (focusing on the bacteria and viruses) transport and retention in porous media. Because biocolloids are living organisms, their transport in the subsurface is more complex than is the case for abiotic colloids [6]. Not only are they subject to the same physicochemical phenomena as are colloids, but there are also many strictly biological processes that affect their transport, for example: temporal changes in surface properties due to changes in metabolic state, and predation by other subsurface organisms [6]. Therefore, in this review, we focus on the basic science of physical, chemical and biological processes involved in the

†To whom correspondence should be addressed.
E-mail: chenjunhang@haut.edu.cn, gwang198@gmail.com, wenjuliu@haut.edu.cn

transport of biocolloid (e.g., bacteria and viruses) in porous media. Transport of other microorganisms (e.g., spores) is often treated by considering similar approaches, but will not be considered in detail in this work. Modeling of biocolloid transport and deposition is explained along with the factors influencing the biocolloid transport and deposition, and research methods at different scales are reviewed. The information presented in this review is intended to be illustrative and is not exhaustive.

BIOCOLLOID TRANSPORT AND RETENTION IN POROUS MEDIA

Biocolloids possess a high sorption capacity of contaminants owing to their high surface area per unit mass [35]. In groundwater, biocolloids are formed because of the gradient in geochemical parameters such as pH and ionic composition that induce supersaturation and precipitation of solid particles. These biocolloids can also be formed when the concentration of ionic metal species is higher than their solubility limit [36]. Suspended biocolloids are subject to aggregation, filtration and settling. However, these processes are strongly dependent on the density, size and surface chemistry of the biocolloids [3,37]. The stability of biocolloids is controlled by both electrostatic repulsive forces and van der Waals attractive forces. Under electrostatic repulsion, especially at low ionic strength, biocolloids are present in a dispersed state and thus are stabilized [3]. On the other hand, when van der Waals attractive forces are dominant, coagulation is observed. Coagulation (aggregation) occurs due to the destabilization of biocolloidal particles and is dependent on the concentration and size of the particles, which can affect the extent of their collisions. Thus, it is essential to coat biocolloidal particles with a chemical sticky layer, which can allow them to agglomerate (flocculate) and settle down within a reasonable time period. However, the destabilized biocolloids (aggregates) can still be transported through subsurface layers if the aggregates are sufficiently small compared to the void space between solid surfaces [3].

1. Mechanisms Responsible for Biocolloid Transport and Retention in Porous Media

1-1. Biocolloid Transport Mechanisms to the Porous Media Surface

Several processes, such as advection, diffusion and dispersion, that influence the solute transport in porous media can also affect biocolloid transport. Advection is the movement of colloids along the fluid's streamline trajectory. Under this movement the biocolloids move within the pore water, and the velocity profile is nearly parabolic (Fig. S2). Faster streamline movements occur in the center of the pore throat, while slower streamline movement occurs along the air-water interfaces (AWI) and/or solid-water interfaces (SWI) [38]. Therefore, colloids are transported faster near the center of the streamline as compared to their movement along the SWI and AWI. However, the tortuosity of the path through the porous media and the heterogeneity of the fluid velocity might result in the dispersion of biocolloids [39]. In addition, colloid diffusion can occur due to random interactions among particles leading to Brownian movements [26].

Three dominant transport mechanisms of suspended colloid (including biocolloid) transport towards a collector surface are shown in Fig. 1. The theoretical framework of these transport mechanisms was proposed by Yao et al. [40] and Rajagopalan and Tien [41], and has been improved by others, particularly by Rajagopalan et al. [42] and Ryan and Elimelech [43].

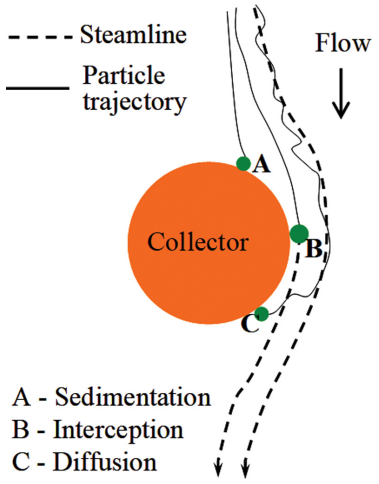

Fig. 1. Mechanism of colloid transport towards a collector surface (adapted from Yao et al. [40]).

Gravitational sedimentation (case A in Fig. 1) occurs if colloid density is much higher than that of water. This results in the colloids following a different trajectory than the streamline flow due to the force of gravity. The colloids, thus, are settled out of the suspension and deposit on the porous media surface. *Interception* (case B in Fig. 1) can occur when the distance between the streamline path and collector surface is smaller than the radius of the colloid. *Diffusion* (case C in Fig. 1) is a process by which a colloid in suspension is transported to the collector surface because of Brownian diffusion.

1-1-1. Size Exclusion

Size exclusion occurs when the colloids are transported faster than the conservative tracer in the porous media, owing to the difference in their respective sizes [6]. When colloids are excluded from the small pore spaces between the solid surfaces, it leads to faster colloid transport than that of the conservative tracer [44].

Fig. 2 illustrates the flow of water and transport of colloids under saturated and unsaturated conditions. As seen in Fig. 2(b), flow and

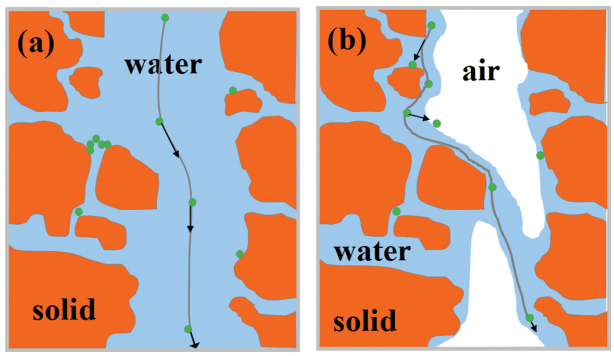

Fig. 2. Illustration of colloid (green circle) transport processes in saturated (a) and unsaturated (b) porous media (adapted from Kretzschmar and Schäfer [45]).

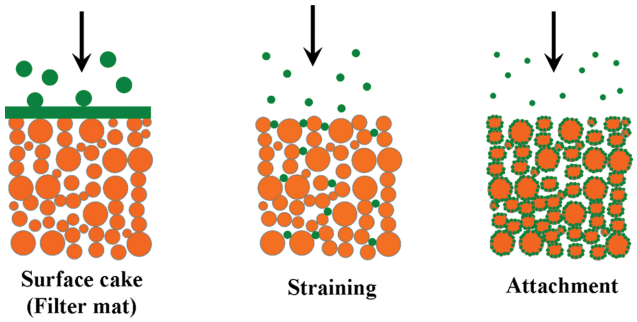

Fig. 3. Three main mechanisms of biocolloid deposition (adapted from McDowell-Boyer et al. [35]).

colloid transport in the unsaturated condition is more complex than in saturated condition (Fig. 2(a)), due to the presence of the air and flow discontinuities.

1-2. Biocolloid Deposition Mechanisms through Porous Media

Some of the biocolloids might be retained on the surface when they pass through the porous media. Three main mechanisms of biocolloid deposition, including mechanical (surface) filtration, straining and attachment (physicochemical filtration) [35], in saturated porous media are shown in Fig. 3.

1-2-1. Mechanical Filtration

When the size of the suspended particles is larger than the size of the pore channels in the porous media, a surface cake or filter mat is formed at the inlet end of the pore throat. As the accumulation of particles increases, the thickness of the surface cake also increases, resulting in a decrease in the permeability of the porous medium-filter cake system [46].

1-2-2. Straining

Straining occurs when the colloids are small enough to enter the porous media and cannot be mechanically removed in down-gradient pore throats. The reason is that the colloids cannot get through the crevices formed by grain-to-grain contacts of the porous media[47] (see Fig. S3).

Herzig et al. [48] reported straining from a geometric standpoint and observed that when the ratio of the diameter of the colloid particle to the median grain diameter of the porous media was higher than 0.05, straining was significant. However, a recent work reported that straining can be considered even when the ratio of the diameter of colloid particle to the median grain diameter of the porous media is as low as 0.0017 [44,49-51]. It is suggested that straining is depth-dependent, with large amount of straining observed at the textural interfaces of porous media with decreasing grain size [44,52,53]. This observation has also been confirmed by a micro-model on a pore scale, by using bacteria and latex microspheres [54-57]. Note that the oversimplification of the size and shape distribution of the complex nature of pores and colloids might result in a discrepancy between the experimental data and numerical simulations and geometric calculations [58]. The shape of bacteria can range from rod to ellipsoidal and to spiral, and due to the wide range of grain sizes and surface roughness, the pore size of porous media can span over several orders of magnitude [58]. Therefore, careful consideration of this fact is necessary during any experimental analysis of the phenomenon.

1-2-3. Clogging

Clogging may be due to the accumulation of stable solid materials between the porous media [32]. The process of clogging may be caused by an improper balance of the intricate microorganism population within the filter, excretion of extracellular polymeric substances (EPS) by some bacteria, and accumulation of biomass from growth of the microorganisms [32]. Filtration of wastewater involves the development of pore clogging, mainly at the infiltration surface, but also deeper in the filtration media [32]. Building up of biofilm may restrict pore sizes and thus enhances the effect of straining. There is much experimental evidence that particle removal is more efficient in clogged porous media [59-61].

1-2-4. Attachment at Solid-water Interfaces (SWI)

Very small colloid particles relative to the pore size of the porous media results in the attachment of the colloids at SWI due to the physicochemical and biological interactions between the porous media and colloids (Fig. S4) [35]. Filtration theory can predict the efficiency of biocolloid attachment by considering Derlaguin-Landau-Verwey-Overbeek (DLVO) forces between biocolloids and porous media, which describes the interactions between colloids and SWI with van der Waals and electrical double layer forces. The attractive van der Waals force is related to the colloid and collector surface properties, while electrical double layer force can be attractive or repulsive depending on the relative charges of the colloid and collector.

Attachment of biocolloids on SWI has been widely reported by column flow experiments [62-65]. And it was suggested that biocolloid removal efficiency attachment on SWI is dependent on many factors, such as solution chemistry, surface properties of biocolloids and grains, which will be discussed in detail in Section 2.3.

Studies have suggested that biocolloid attachment on SWI not only occurs in saturated porous media, but also in unsaturated conditions [49,66-69]. In unsaturated porous media, water flow is restricted to the smaller regions of the pore space through capillary forces [58]. Thus, in addition to the retention mechanism observed in saturated porous media, including attachment onto SWI and straining, in unsaturated porous media colloid deposition can be influenced by attachment at air-water interfaces (AWI) [70,71], by film straining in water films enveloping the solid phase [72,73] as well as by attachment at air-water-solid interfaces (AWS) [74-77].

1-2-5. Attachment at Air-water Interfaces

The AWI can serve as the collector of colloids under unsaturated conditions (Fig. S5). Based on the study by Wan and Wilson [70], the interaction between colloids and AWI has been considered as the dominant colloid retention process [70]. They found the attachment of bacteria on AWI in a glass micromodel under epifluorescence microscope and observed that hydrophobic particles displaying strongest affinity to both the AWI and the glass was due to lower charge density on the hydrophobic surface. Positively charged particles displayed a stronger affinity to the AWI compared to negatively charged particles. To study retention at the AWI, numerous studies have been conducted using etched-glass micromodels for visualization. In these micro-model tests, a wide variety of colloids, such as clay particles, hydrophilic and hydrophobic latex microspheres, as well as bacteria have been used.

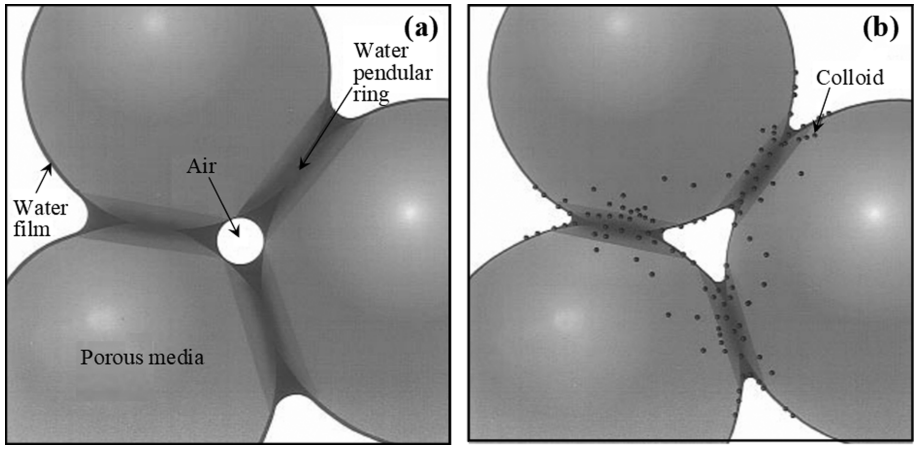

Fig. 4. Conceptual diagram of unsaturated straining: (a) Pendular rings are at the verge of disconnecting, and (b) Pendular rings disconnected (connected only by thin films) and colloids are retained in the pendular rings and in water films (taken from Wan and Tokunaga [73]).

1-2-6. Film Straining

In unsaturated porous media, water flow is observed in narrow, water-filled pores and in pendular rings or water films retained owing to the capillarity in the grain-grain interfaces [26,73,78]. A pendular ring refers to the water held by surface tension near the adjacent grains in contact [73]. Wan and Tokunaga introduced the concept of film straining (Fig. 4), which is considered as an another mechanism of colloid deposition under unsaturated conditions [73].

According to Wan and Tokunaga [73], film straining is dependent on the probability of pendular ring discontinuity as well as on the ratio of the size of colloid to the thickness of the film. With the decrease in capillary pressure, such as during the draining of porous medium, the discontinuity probability of pendular ring increases from 0 to 1. As pendular rings disconnect and increased proportion of water flow occurs, colloid transport is relegated to the adsorbed films of water that envelop the grains [73]. Water films of the order 20-40 nm were observed and it was suggested that film straining can occur when water film thickness is smaller than the colloid diameter (Fig. 5) [73].

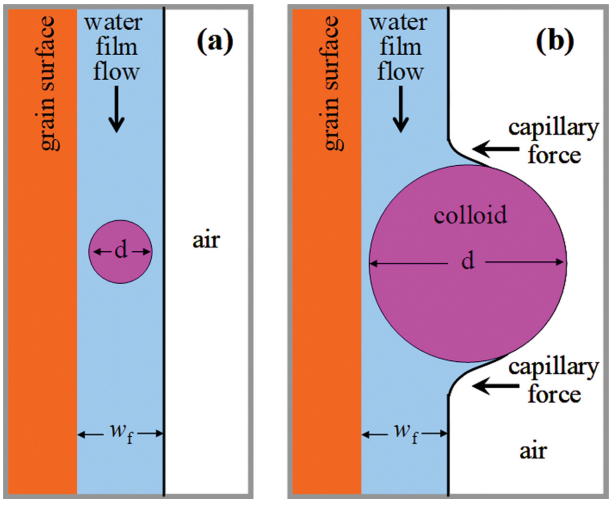

Fig. 5. Conceptual diagram of a close-up view of the thin water film region in Fig. 4(b). (a) When the diameter of the colloid particle, d, is smaller than the thickness of the water film (w_f), film straining is not efficient; (b) when d is larger than w_f, film straining occurs (adapted from Wan and Tokunaga [73]).

1-2-7. Attachment at Air-water-solid Interfaces

In unsaturated porous media, colloids can be retained at the area of contact of AWI and SWI, referred to as AWS or AWmS attachment [74-77]. Zevi et al. proposed the term "air-water meniscus-solid (AWmS)" [76], which is the region where the water meniscus diminishes into a thin water film on the grain surfaces (Fig. S6). It has been reported that hydrophilic colloids tend to retain at the AWI in unsaturated silica sand flow chambers [74,75].

2. Biocolloid Transport and Deposition Modeling

When a sorbing porous medium is considered, the total amount of the contaminant M in the soil can be represented in the following form, based on the mass conservation law:

$$M=\rho_b s+\theta C \tag{1}$$

where, ρ_b is the bulk density of porous medium [$M\cdot L^{-3}$], s is the solid phase concentration on the porous medium [$N_c\cdot M^{-1}$, where N_c is biocolloid counts], and C is the concentration in the liquid phase [$N_c\cdot L^{-3}$].

When the concentration of the contaminant on the porous medium is included in the advection-dispersion equation (ADE), the general transport equation for contaminant, commonly accounting for microorganism transport and fate, can be written as follows [58]:

$$\frac{\partial \theta_c C}{\partial t}+\rho_b\frac{\partial S}{\partial t}+\frac{\partial A_{aw}\Gamma}{\partial t}=\frac{\partial}{\partial z}\left(\theta_c D\frac{\partial C}{\partial z}\right)-\frac{\partial q_c C}{\partial z}+B_w \tag{2}$$

where, C is the microbe concentration in the aqueous phase [NL^{-3}], S is the microbe concentration retained on the SWI [NM^{-1}], Γ is the microbe concentration retained on the AWI [NL^{-2}], θ_c is the volumetric water content accessible to microbes [L^3L^{-3}], D is the hydrodynamic dispersion coefficient for microbes [L^2T^{-1}], ρ_b is the bulk density [ML^{-3}], A_{aw} is the air-water interfacial area per unit volume [L^2L^{-3}], q_c is the volumetric water flux density for colloids

[LT^{-1}], B_w represents growth/death of the microbes in the water phase [$NL^{-3}T^{-1}$], z is the distance in the vertical direction [L], and t is the time [T].

Biocolloid removal from the liquid to solid phase can be modeled as equilibrium or kinetic processes that are irreversible or reversible. According to Bradford et al. [58], exchange of microbes with the SWI and AWI can be divided into equilibrium sorption, attachment and straining mechanisms as:

$$\rho_b\frac{\partial S}{\partial t}=\rho_b\frac{\partial S_{eq}}{\partial t}+\rho_b\frac{\partial S_{att}}{\partial t}+\rho_b\frac{\partial S_{str}}{\partial t}-B_s \tag{3}$$

$$\frac{\partial A_{aw}\Gamma}{\partial t}=\frac{\partial A_{aw}\Gamma_{eq}}{\partial t}+\frac{\partial A_{aw}\Gamma_{att}}{\partial t}+\frac{\partial A_{aw}\Gamma_{str}}{\partial t}-B_a \tag{4}$$

where the subscripts of eq, att and str denote microbe concentrations retained by equilibrium sorption, attachment and straining, respectively, B_s and B_a are the microbes growth/death on the solid phase and at the air-water interface, respectively [$NL^{-3}T^{-1}$].

A general nonlinear equilibrium expression (describing interactions between solid phases and solutes as well as the biocolloid retention) for biocolloid sorption, which can be incorporated into Eq. (3) is shown as [79]:

$$S_{eq}=\frac{K_d C^{\beta}}{1+\xi' C^{\beta}} \tag{5}$$

where β, K_d and ξ' are empirical coefficients. And a similar expression to Eq. (5) can be used to account for sorption on the AWI by replacing S with Γ.

Biocolloid mass transfer between the aqueous and SWI and AWI due to attachment and detachment can be modeled as follows [80]:

$$\rho_b\frac{\partial S_{att}}{\partial t}=\theta_c\psi_{sw}k_{asw}C-\beta_b k_{dsw}S_{att} \tag{6}$$

$$\frac{\partial A_{aw}\Gamma_{att}}{\partial t}=\theta_c\psi_{aw}k_{aaw}C-A_{aw}k_{daw}\Gamma_{att} \tag{7}$$

where k_{asw} and k_{dsw} are the first-order colloid attachment and detachment coefficient to the SWI, respectively [T^{-1}]; k_{aaw} and k_{daw} are the first-order colloid attachment and detachment coefficient to the AWI, respectively [T^{-1}]. Ψ_{sw} and Ψ_{aw} are a dimensionless colloid retention function on the SWI and AWI to account for blocking or ripening.

Classical colloid filtration theory (CFT) is commonly employed to evaluate the colloid attachment rate in saturated porous media as [15,17,40]:

$$k_{asw}=\frac{3(1-\theta)\upsilon}{2d_m}\alpha_s\eta_0 \tag{8}$$

where, d_m is the median grain diameter [L], α_s is the total sticking efficiency [-], and η_0 is the single collector contact efficiency [-]. However, the classical colloid filtration theory was originally developed to describe colloid behavior under favorable attachment conditions and in this case α_s equals to 1 [27].

Colloid filtration theory predicts that the deposition profile of retained bacteria with transport distance is an exponential distribution [40,81]. However, many researchers observed a hyper-exponential distribution rather than an exponential distribution for deposition profile in porous media under unfavorable attachment conditions (existence of energy barrier). A variety of hypotheses have been reported to explain these experimental observations. Some of the explanations have been attributed to soil surface roughness [82], hydrodynamic drag [83], charge variability of porous media [84] or heterogeneity of the colloid surface charge [85]. Other researchers have suggested that these discrepancies exist because colloid filtration theory does not account for *straining*, which is based on pore structure.

Several researchers have divided the sites of colloidal sorption into two fractions and assumed that at each sorption site, different rates or processes can occur [49,86]. Mass transfer, described by the conventional attachment and detachment model using site 1 and site 2, was employed to describe the straining processes (depth-dependent) of bacterial deposition behavior [49,87].

Thus, the mass transfer rate of colloids (bio-colloids) between aqueous phase and solid phase can be represented as [44]:

$$\rho_b\frac{\partial S_{att}}{\partial t}=\theta_c\psi_{sw}k_{asw}C-\beta_b k_{dsw}S_{att}+\theta_c\psi_{str}k_{str}C \tag{9}$$

$$\psi_{str}=H(z-z_0)\left(1-\frac{S_{str}}{S_{str}^{max}}\right)\left(\frac{d_m+z-z_0}{d_m}\right)^{-\Omega} \tag{10}$$

where, k_{str} is the first-order coefficient for straining [T^{-1}]; ψ_{str} accounts for depth-dependent deposition, which are dimensionless retention functions; d_m is grain median diameter [L]; $H(z-z_0)$ is the Heaviside function, z_0 is the coordinate of the location where the straining process starts; S_{str}^{max} is the maximum solid phase concentration of strained colloids, and Ω is an empirical factor which controls the retention profile shape [-].

Wan and Tokunaga [73] proposed a kinetic formulation to simulate film straining behavior in unsaturated porous media as:

$$\frac{\partial(A_{aw}\Gamma_{str})}{\partial t}=\theta_c\omega_{str}C \tag{11}$$

with

$$\omega_{str}=\omega_t P_d\left(\frac{d_b}{d_f}\right)^{\zeta} \tag{12}$$

where ω_{str} is the film straining rate coefficient [T^{-1}], P_d is the probability of pendular ring discontinuity [-], d_b is the microbe diameter [L], d_f is the thickness of the water films, and ζ [-] and ω_t [T^{-1}] are empirical parameters.

Incorporation of biological factors into predictive mathematical models for the transport and fate of biocolloids is still a challenge, and the net rate of pathogen growth, death and inactivation in the water, solid and air phases can be presented as [58]:

$$B_w=\theta_w(\Lambda_w-X_w)C \tag{13}$$

$$B_s=\rho_b(\Lambda_s-X_s)S \tag{14}$$

$$B_a=A_{aw}(\Lambda_a-X_a)\Gamma \tag{15}$$

where subscripts w, s, a denote the water, solid and air phases, respectively. X is the coefficient of death/inactivation [T^{-1}], Λ is the microbe growth coefficient [$NL^{-3}T^{-1}$].

The inactivation coefficient may be given as (the Weibull model)

[88]:

$$X_w(t) = mb^{-m}t^{m-1} \quad (16)$$

where b_w [T] and m [-] are empirical parameters.

The growth/survival coefficient can be given as [58]:

$$\Lambda_w(C) = \Lambda_0(1 - C/C_{max}) \quad (17)$$

where Λ_0 is the growth rate in the absence of competition [T^{-1}], and C_{max} is the maximum concentration that is associated with the upper limit of population growth.

Analytical biocolloid transport models, although limited by many assumptions, are important tools for preliminary estimation of biocolloid transport, examination of possible boundary conditions, validation of numerical solutions and determination of biocolloid transport parameters from experiments [89]. Chrysikopoulos and colleagues developed several one-dimensional and three-dimensional mathematical models for biocolloid transport in homogeneous saturated porous media and heterogeneous porous formations, which also accounts for virus sorption and inactivation of liquid phase and adsorbed viruses with different time dependent rate coefficients [89-94]. And they reported that multidimensional contaminant transport models have several advantages over one-dimensional models. For example, multidimensional models can account for concentration gradients and contaminant transport in directions perpendicular to the groundwater flow [89].

3. Factors Affecting Biocolloid Transport and Retention

Several important factors controlling the transport and retention processes of biocolloids in porous media have been explored by many theoretical and experimental investigations, recently. These factors include porous medium characteristics such as grain and pore size; soil type and structure; the presence of surface coatings; chemical factors (solution chemistry) like ionic strength, valence and pH; hydrodynamic properties such as water content and pore water velocity; and various biological properties such as cell size and shape, motility, growth phase, hydrophobicity, surface charge and biofilm.

3-1. Factors Linked to Porous Medium Characteristics

3-1-1. Grain Size and Pore Size as Well as their Distribution

Among the various physical factors that influence colloidal transport and retention in porous media, including that of bacteria, the media grain size and pore size as well as their distribution are considered as critical parameters. Median grain size and uniformity coefficient are often used to describe granular media in subsurface and engineered filtration systems. Grain size can be described by the median (d_m) or effective (d_{10}) size of granular media used in filtration applications, which represent the grain diameter at which 50 or 10 percent of the media by mass are smaller, respectively [95]. The uniformity coefficient of the media is described by d_{60}/d_{10} which indicates the heterogeneity of the media grain sizes [95]. The lower the value of the uniformity coefficient, the more uniform is the material [95]. The angularity and roughness of media grains also substantially affect the pore size between media grains and impact the contact opportunities between microorganisms and porous media surfaces [96,97]. In the existing literature, it has widely been reported that grain or pore size of porous media can influence bacterial transport. Gargiulo et al. [98] observed that bacterial retention increased when the size of sand particles decreased, with most of the bacteria retained at the inlet side of the column. Chrysikopoulos and Aravantinou [69] reported the role of three different sand grain sizes on virus attachment (ΦX174 and MS2), and in most of the cases considered, bacteriophage attachment was shown to decrease with increasing quartz sand size. However, Bolster et al. [85] claimed the influence of grain size on bacterial retention to be insignificant. It is to be noted that most of the previous studies have focused on bacterial transport and retention in homogeneous porous media [99,100]; however, much information is also available on heterogeneous porous media with different pore size geometry [19,101]. Different grain sizes imply different pore sizes, which can affect the colloidal transport. Recent studies have reported that pore size as well as their distribution can influence biocolloid transport and retention in porous media [102-105]. Even though the effect of pore size has been extensively investigated, a limited number of studies reported the effect of pore size distribution in the porous media on the transport and retention of colloids (including bio-colloids) [19]. Preferential transport of colloids (bacteria) through macropores has been observed in heterogeneous porous media, which is constituted of macropores added into the homogeneous sand matrix [106,107]. Colloidal transport and deposition in real soils, which has a complex geometry, has been reported by other researchers [19,108]. However, in complicated real porous systems controlled by the hydrodynamic conditions, it was difficult to reach conclusive results concerning colloidal/biocolloidal transport. Leij and Bradford [109] investigated the transport of latex microspheres in porous media which constituted a mixture of different grain size sands under laboratory scale conditions. However, definitive conclusions with respect to the colloidal transport parameters could not be drawn from the study because of the complex flow pattern in the porous media and the relatively small size of samples. Thus, the effect of different grain sizes or pore size distributions is more apparent at lower loading rates and in groundwater environments, which requires further investigation [110].

3-1-2. Soil Type and Structure

One study reported the use of ten different soil samples from New Zealand for the leaching experiments to elucidate the parameters determining microbial (*Salmonella typhimurium* 28B) transport and attenuation [111]. It was concluded that with the increase in leaching vulnerability, the general pattern of mobile water content was increased, which suggested that the structure of soil plays an important role in microbial transport. Jiang et al. [112] examined the ability of six undisturbed soil samples, through lysimeter, to remove bacteria under field conditions, and examined the dynamic changes of the soil structure. It was observed that the soils with higher topsoil clay content had a high risk of bacteria leaching in the soils through preferential flow paths. The effect of soil texture on *Escherichia coli* NAR and bromide transport through the columns packed with two-texturally different soils (clay loam and sandy loamy) was studied by Safadoust et al. [113]. In this case, a higher attachment coefficient of bacteria in the fine textured clay soil was observed. Also, increased clay content was reported to enhance both pore network formation and soil structure, resulting in enhanced transport of biocolloids in structured clayey soils,

which was more than that observed with the sandy soils.

3-1-3. Fractured/Macroporous Media

Subsurface formations are not uniform and homogeneous porous media, several formations are fractured, which can result in preferential flow. There are two porosity-permeability systems for fractured media: one makes up the pore space between the grains, which exhibits lower permeability (accounting for the largest void space fraction); the other makes up the pore space of the fractures and fissures (macropores), which exhibit higher permeability (accounting for the smallest void space fraction) [114]. The presence of preferential flow paths generally reduces biocolloid removal due to faster transport [115]. Brennan et al. [116] investigated bacteria (*E. coli* IND1) as related to flow patterns visualized by the tracer (brilliant blue) in grassland soils, and they concluded that vertical bacterial transport mainly occurs in preferential flow paths.

3-1-4. The Presence of Surface Coating

Bolster et al. [85] reported that the metal-oxyhydroxide coated aquifer sediments could result in positively charged surfaces of sediment, and this could increase the colloid deposition rates because bacteria are negatively charged at typical groundwater pH values. Kim et al. [117] reported a decrease in bacterial mass recovery when the content of Al-/Fe-coated sand increased. On the other hand, Dong et al. [118] concluded that the attenuation of the bacteria *Comamonas* sp. was mainly influenced by the grain size of porous media rather than by the presence of iron and aluminum hydroxide coatings.

3-1-5. The Effect of Heterogeneity

Natural aquifers may have different types of heterogeneities across different scales [119-122]. And these heterogeneities may commonly be classified into mainly four groups: (a) nano- and microscale heterogeneities, arising from variations in the porous media surface roughness which can affect particle deposition [123,124]; (b) chemical heterogeneity originating from diversity in the porous media surface charge and it can also affect particle deposition [125, 126]; (c) pore-to continuum heterogeneity emanating from variations in skeletons and pore dimensions, such heterogeneity may result in preferential flow pathways at the pore scale [127,128]; (d) stratigraphic heterogeneity, commonly found in geological formations, results from variation in the grain type from one layer to another [129,130]. Mahmoudi et al. [131] investigated the impact of stratigraphic heterogeneity and release pathway on the bacteria transport in porous media, and they observed that within single-layer systems, resembling stratigraphically homogeneous natural porous media but with two types of natural heterogeneities (textural and pore to continuum heterogeneities), *E. coli* tends to transfer faster than tracer solute. Moreover, mono-pulse breakthrough curves in both single-layer and multi-layer systems generally exhibited multiple peaks, attributed to preferential flow pathways, polydispersity and aggregation in the population of *E. coli*. Bradford et al. [123] reported a comparison of types and amounts of nanoscale heterogeneity on bacteria retention, and their observation demonstrated that chemical heterogeneity and nanoscale roughness play a critical role in controlling irreversible bacteria retention. In particular, spatial variations in metal oxide coatings, and especially nanoscale roughness, have important roles in determining bacteria retention on natural surfaces. The relative importance of the various heterogeneity types was found to change with the solution ionic strength and specific ranges in considered heterogeneity parameters.

3-2. Factors Linked to Solution Chemistry

3-2-1. Solution Ionic Strength, Valence and pH

It has been reported that the ionic strength of a solution can affect bacterial retention in porous media. With the increase in ionic strength from 10-100 mmol/L at a pH of 5.6-5.8, bacterial deposition has been observed to increase [132]. Another research reported an increase in bacterial deposition with increasing ionic strength at pH=5.8, which decreased at a pH of 8.4 and 9.2 [133]. Similar observations were also reported by other authors who found that increasing ionic strength can result in higher bacterial attachment at a pH of 5.8-7.2 [134-137]. However, Haznedaroglu et al. reported that bacterial deposition was not influenced by ionic strength ranging from 1 to 100 mmol/L [138]. It was reported that divalent cations such as Ca^{2+} can act as a bridge, interacting with charged functional groups on cell surface, resulting in greater bacterial deposition in porous media [132]. Janjaroen et al. observed that the attachment of oocysts on a Suwannee river natural organic matter-coated surface was lower in the Mg^{2+} solution than that in the Ca^{2+} solution, while oocysts deposition on the surface of quartz sand was the same with both Mg^{2+} and Ca^{2+} solutions [139]. Another study reported a series of experiments with different valences (KCl and $CaCl_2$) to analyze the effect of solution chemistry on bacterial deposition, and observed that higher valence results in higher bacterial deposition [132]. Bacterial deposition can be also affected by the pH of the solution, with increased bacterial retention reported with reduced pH [140]. However, it is also reported that bacterial deposition is not affected within the range of pH from 5.5 to 7.0 and from 4.0 to 9.0, as observed by Jewett et al. [141] and Stenström [142]. Therefore, since the groundwater pH is near neutral and the ionic strength of groundwater is less than 10 mmol/L, the variations in ionic strength and pH are insignificant for bacterial retention under typical environmental conditions [28].

3-3. Factors Linked to Hydrodynamic Properties

3-3-1. Water Saturation

Most of the experimental and theoretical studies of particle transport are focused on saturated porous media. Less is understood about transport in unsaturated porous media due to the systematic complexity that arises with the presence of an air phase [58]. The transport and deposition of colloids depends significantly on the water saturation in porous media. For a given pressure gradient, the rate of water flow is higher in saturated porous media than that under unsaturated conditions. In fact, at lower saturation, the effective (water-filled) porosity is decreased and the channel conducting water is reduced.

Various studies have suggested that water saturation plays a key role in biocolloid retention in vadose zone, with a decrease in water saturation resulting in an increase in biocolloid retention. Sim and Chrysikopoulos [143,144] investigated the effects of soil moisture variation on virus sorption at the liquid-solid as well as air-liquid interfaces, and they found that at low soil moisture, virus removal is significantly enhanced due to the irreversible adsorption of viruses onto the air-liquid interface. Anders and Chrysikopoulos [145] reported that saturation levels can affect virus transport through porous media, and the liquid to liquid-solid and liquid to air-liq-

uid interface mass transfer rate coefficients were shown to increase for both bacteriophage as saturation levels were reduced. This can be explained by following reasons: 1) With lower saturation, the diffusive length is reduced, resulting in an increased attachment to SWI [146]. According to Ginn et al. [6], colloid tends to travel shorter distance in lower saturated soils than under higher saturated conditions; 2) At lower saturation, the area of air-water interface is enlarged, resulting in more colloid attachment to this interface [70,147]; 3) The trapping of colloids in the thin water films because of film straining is increased at lower water saturation [73,78].

3-3-2. Pore Water Velocity

It has been reported that colloid transport and deposition is related to water velocity, with deposition efficiency and detachment rate of colloids changing by the hydrodynamic forces exerted on the colloids [83,148-150]. Increased pore water velocity can result in decreased colloid deposition. Johnson et al. [151] found that increasing pore water velocity can lead to decreased colloid deposition. Similar results were also observed by Keller et al. [149] and Elimelech et al. [152]. These authors reported that increasing pore water velocity could result in an increase of hydrodynamic drag, which can decrease colloid deposition. The main reason for this observation has been attributed to the increase in hydrodynamic drag with increase in pore velocity, which can decrease colloid deposition. Kokkinos et al. [153] evaluated the effect of pore water velocity on human adenovirus transport in water-saturated columns, and they concluded that although the virus mass recovery and degree of velocity enhancement were affected by the interstitial water velocity, no clear trends could be determined.

3-4. Factors Linked to Biological Properties

3-4-1. Cell Size and Shape

Bacteria constitute a vast domain of prokaryote microorganisms varying widely in shape and size. Typically, bacteria with an average width of around 0.25-2.0 μm and length of 1-10 μm, display three basic shapes: rod (bacilli), round (cocci) and spiral (spirilla). It is reported that the size and shape of bacteria can affect bacterial transport and deposition in porous media. The cell surface properties of 19 bacterial strains were also reported to influence bacterial transport through loam soil [154]. It was observed that cells smaller than 1 μm in length were more effectively transported than those longer than 1 μm. Another research reported that bacteria with larger sizes were retained in porous media [155]. To examine the influence of cell shape on bacterial transport, Weiss et al. [156] conducted transport tests with 14 strains and observed that spherical shape was more liable to transport in porous media.

3-4-2. Motility

Motility is recognized as a significant biological character of certain bacteria and there are a variety of ways used for the determination of bacterial motility [157]. Two of the most commonly used methods are the slide method and soft agar stabbing (tube method). In the slide method, one droplet of bacterial culture is suspended from a glass coverslip over a microscope slide and then observed with a light microscope. If the bacterial cells are observed to be actively moving and tumbling, they are considered as motile, while those showing only Brownian movement are considered as non-motile cells [158].

Motile bacteria have specialized structures called flagella, which helps in their motility [159]. The flagellum is usually 10-20 nm in width and 15-20 μm in length [34]. Mobile bacteria have a better chance to overcome electrostatic repulsive forces through their kinetic energy and thus are more prone to contact a possible adhesive surface. However, non-motile bacteria rely on water flow or Brownian motion to move towards the surface of porous media [160]. Although cell wall type and shape have been reported to have minor effects on bacterial transport [161], motility tends to augment the rate of adsorption and to diminish the rate of desorption.

3-4-3. Growth Phase

Batch culture is a commonly used method for the laboratory growth of bacteria. In this case, the bacteria are incubated in a closed vessel with a given volume of nutrients under specific growth conditions. Four distinctive growth phases, including lag phase, exponential phase, stationary phase as well as death phase are observed in batch cultures (Fig. S7). The newly inoculated bacteria require time to adapt to the growing medium and hence show slow multiplication rate. This is called the lag phase. In the exponential phase, cells grow rapidly and are most active in genetic replication. After some time, however, due to limited nutrient supply and accumulation of secreted waste products, cellular growth is inhibited and the cells enter a stationary phase. Here the rate of bacterial growth decreases and no change in cell numbers is observed in such phase. In the death phase, bacteria begin to perish due to starvation or intolerable accumulation of toxic waste products.

Gargiulo et al. [162] examined the influence of bacterial growth phase on the transport and deposition of *Deinococcus radiodurans* in porous media. These cells were harvested during the exponential phase and stationary phase, and it was observed that the cells were metabolically more active and exhibited greater deposition in exponential phase than in the stationary phase. However, another study reported contrasting results, where higher bacterial retention was observed in the stationary phase than in the exponential phase [163]. This was attributed to the fact that high degree of local charge heterogeneity on the outer membranes of bacteria exists in the stationary phase.

3-4-4. Hydrophobicity of Cell Surface

Hydrophobicity of cell surface is an important physicochemical property of the bacteria [164]. Bacteria can adhere to host tissue cells or inert surfaces via hydrophobic effect if the surface has sufficient density of apolar areas [165]. The surface hydrophobicity of bacteria is contributed by certain proteins bonded to their cell wall and membrane. The presence of lipoteichoic acid in the cell wall of *Staph. aureus* is believed to be responsible for its surface hydrophobicity [165]. Various protein constituents on the surface of coagulase-negative staphylococci are also reported to affect their hydrophobicity [166].

Two commonly used methods to quantify the hydrophobicity of bacterial cell surface include *Microbial adhesion to hydrocarbon test* and *Contact angle method*. *Microbial adhesion to hydrocarbon test* was put forward by Rosenberg et al. [167] and later refined by Geertsema et al. [168]. In this method, a suspension of bacteria is mixed with hydrocarbons such as hexadecane and toluene, and the hydrophobicity of cells is determined owing to the fact that the higher number of hydrophobic cells are bound to the hydrocarbons. On the other hand, *Contact angle method* is more suitable to

determine the bacterial cell surface hydrophobicity. One drop of a solvent, such as water, is placed on a smooth lawn of dried cells and the dissipation of the droplet depends on the cell surface hydrophobic properties [169]. Compared to *Contact angle method*, *Microbial adhesion to hydrocarbon test* has the following limitations [170]: 1) *Microbial adhesion to hydrocarbon test* is not standardized and thus the results from different laboratories might show some deviation; 2) The formation of small hydrocarbon droplets can be stabilized by bacteria and they do not leave the water phase, which may influence the measurement; 3) Quantification of hydrophobicity may be affected by the extraction of cell surface components by hydrocarbon liquids.

The influence of hydrophobicity of two bacterial species on their movement through three different granular porous media with different surfaces was investigated [171]. In Fe-coated sandy columns, higher recovery of hydrophilic bacterium with low negative charge was observed, as compared to those with a high negative surface charge. However, in uncoated quartz sand columns, the hydrophobic bacterium with a high negative surface charge showed higher recovery. Gargiulo et al. [49] carried out transport experiments with two bacterial species which were similar in shape, size and surface charge, but different in hydrophobicity of cell surface. It was observed that bacterial deposition increased with the increase in the bacterial surface hydrophobicity.

3-4-5. Surface Charge of Cell

Cell wall components such as phosphates, proteins and amino groups can contribute to the net charge of the bacterial cell surface [172]. It has been reported that at physiological pH, most bacteria have a negative surface charge, which can be due to cell membrane phospholipid bilayer and the presence of polysaccharides within the wall and due to cell membrane macromolecules such as phospholipids [173]. The charge of cell surface can be determined based on electrical potential (zeta potential) of the interfacial region between aqueous and cellular surface. Jacobs et al. [174] studied the effect of cell properties on bacterial attachment to sand. It was concluded that lower negative zeta potential can result in electrostatic repulsions that delay bacterial adhesion, resulting in an enhanced bacterial transport.

3-4-6. Gram Stain Types

Bacterial cell surface is covered with large number of macromolecules (Fig. S8). According to cell wall structure, bacteria are divided into gram-positive and gram-negative cells. Gram-positive cell walls possess a relatively simple structure primarily composed of linear polymers of peptidoglycan [175]. The peptidoglycan polymers are covalently linked together to form a giant molecule (25 nm thick), imparting strength and structure to the cell wall. The peptidoglycan consists of repeated dimers of *N*-acetylglucosamine and *N*-acetylmuramic acids and is rich in carboxyl functional groups [175]. Secondary polymers (teichoic and teichuronic acids) are also present within the peptidoglycan framework and provide additional carboxyl and phosphate functional groups. The cell wall is separated from the protoplast by a lipid/protein bilayer called the plasma membrane. On the other hand, the structure of Gram-negative cell wall is more complex with a thin peptidoglycan layer (~7.5 nm), but devoid of secondary polymers [175]. The peptidoglycan layer is located between plasma membrane and an outer membrane (lipid/protein bilayers). The outer membrane is located above the peptidoglycan, is essentially composed of lipopolysaccharides (LPS) which are rich in carboxyl groups, and has functional groups interacting with dissolved substances in the media [176].

The effect of gram stain type on bacterial transport and deposition was studied by Chen and Walker [177], who concluded that the outer membrane of gram-negative *E. coli*, which primarily contains LPS, can enhance bacterial deposition at low ionic strength. This was because such polymers of cell surface cause "bridging" between bacteria and porous media surface. Another study reported that the length of LPS molecules as well as the characteristic of their charge are not directly related to the kinetics of bacterial deposition [178]. This suggested that the adhesive characteristics of bacteria are controlled by the complex combination of LPS composition and charge heterogeneity of cell surface.

3-4-7. Biofilm and Extracellular Polymeric Substances (EPS)

When bacteria are adsorbed to the surface of porous media for enough time, they can excrete polymers (EPS) which can form a bridge, connecting the cells to the porous media surface and resulting in the formation of biofilm [34]. EPS are a complex mixture of macromolecular polyelectrolytes, consisting of nucleic acids, proteins and polysaccharides [179]. These can serve to anchor bacteria to surfaces through interfacial processes, such as hydrophobic association, covalent or ionic bonding, steric interactions, and dipole interactions [179]. Free EPS that is no longer attached to the bacteria can adsorb to the surface of porous media and create a "conditioning film" before cell attachment. Such conditioning films can change the surface characteristics of porous media and improve porous media's ability to retain bacteria. The growth of biofilm from the surface of porous media into the pore channels can result in the decreased size of pore throat, facilitating straining of bacteria. Dai et al. [180] investigated the effect of biofilm on *Cryptosporidium parvum* oocysts transport and deposition in porous media, and they observed that the biofilm can result in an increase in the hydrophobicity of the porous media. This can result in decreased attachment of the relatively hydrophilic oocysts on the porous media.

3-5. Factors Linked to Coexist with other Colloids

Georgopoulou et al. [181] investigated the influence of graphene oxide nanoparticles (GO NPs) on the cotransport of biocolloids in the saturated porous media, and they found that the presence of GO NPs decreased bacteria mass recovery rates more during their transport than cotransport, suggesting that bacterial coexistence hindered inactivation and deposition processes. Syngouna and Chrysikopoulos [182-184] studied the cotransport of clay colloids and viruses through water-saturated and partially columns packed with glass beads, and they observed that gravity affected viruses and clay colloid cotransport; besides, colloids can facilitate the transport of viruses in saturated porous media. However, under unsaturated conditions, clay colloids facilitated the transport of ΦX174 while hindered the MS2 transport. Katzourakis and Chrysikopoulos [185] developed a 3D mathematical model for virus-colloid cotransport, and experimental data of bacteriophage-clay cotransport were satisfactorily fitted. Syngouna et al. [63] investigated the effect of flow velocity on the cotransport of human adenoviruses with clay colloids and TiO_2 nanoparticles in saturated porous media.

They observed that adenovirus retention by packed columns was highest in the presence of TiO_2 nanoparticles, and no distinct relationship between adenovirus retention and flow rate was established. Bellou et al. [186] reported the interaction of human adenoviruses and coliphages with two different phyllosilicate clays (kaolinite and bentonite) in the packed columns; they concluded that temperature played a significant role in virus adsorption onto clay, and for most cases considered, human adenovirus adsorption is higher at the highest ionic strength.

DIFFERENT FORCES ACTING ON BACTERIA TRANSPORT AND DEPOSITION

Colloid retention is affected by different interactions between colloids and collector surfaces. The Derjaguin-Landau-Verwey-Overbeek (DLVO) theory, which describes the interaction energy as a sum of electrostatic and van der Waals interactions, has been widely employed to describe the interactions between colloids (including bio-colloids) and collector surfaces. However, this theory poorly characterizes short-range "non-DLVO" forces (including hydrophobic [71,187], capillary [73,184], hydrodynamic [83], steric and structural forces), many of which are still incompletely understood.

1. DLVO and Extended DLVO (XDLVO) Interactions

The interaction forces between colloids and collectors are believed to be the dominant forces responsible for colloid deposition in porous media. The total interaction energy Φ_{tot}, typically employed to characterize the colloidal deposition include van der Waals forces Φ_{VDW}, and electrostatic double layer interactions Φ_{EL}, and was described by the classic DLVO theory.

The Φ_{tot} was determined by modeling the microbial cell-porous media system as a sphere-plate interaction [188]. The Φ_{VDW} was determined by the following equation [189]:

$$\Phi_{VDW}(\mathrm{h}) = -\frac{\mathrm{A}}{6}\left[\frac{2(\mathrm{H}+1)}{\mathrm{H}(\mathrm{H}+2)} + \mathrm{In}\left(\frac{\mathrm{H}}{\mathrm{H}+2}\right)\right], \text{ and } \mathrm{H} = \frac{\mathrm{h}}{\mathrm{a}_p} \quad (9)$$

where, Hamaker constant $A=6.5\times10^{-21}$ J and -1.05×10^{-20} J used for bacteria-water-porous media system [188] and bacteria-water-air system [177], respectively; a_p is the particle radius (m); h is the separation distance (m).

The Φ_{DL} can be represented by the following expression:

$$\Phi_{DL}(\mathrm{h}) = 64\pi\varepsilon_0\varepsilon_r\mathrm{a}_p\left(\frac{\mathrm{kT}}{\nu_e\mathrm{e}}\right)^2\gamma_1\gamma_2\exp(-\kappa\mathrm{h}), \text{ and } \gamma_i = \tanh\left(\frac{\nu\mathrm{e}\xi_i}{4\mathrm{kT}}\right) \quad (10)$$

The κ value is calculated by taking the inverse of Debye length:

$$\frac{1}{\kappa} = \sqrt{\frac{\varepsilon_0\varepsilon_r\mathrm{kT}}{2000\cdot\mathrm{N}_A\mathrm{e}^2\mathrm{I}}} \quad (11)$$

where, ε_r and ε_0 are the relative dielectric permittivity of water at 25 °C (78.55) and under vacuum (8.854×10^{-12} C/(Vm)), respectively; T is the absolute temperature (K); k is Boltzmann constant (1.38×10^{-23} J/K); e is the electron charge (1.602×10^{-19} C); ν_e is the valence of the electrolyte; ξ_i is the zeta potential of bacteria/porous media/air bubbles (V), N_A is the Avogadro constant (6.022×10^{23}); $1/\kappa$ is Debye length; I is the ionic strength of the electrolyte (mol/L).

An energy profile of DLVO interaction is constructed by Φ_{tot} as a function of the separation distance between collector surface and colloid (Fig. S9). When the interactive surfaces are like-charged, the double layer force is repulsive and a typical DLVO energy profile is characterized by the primary minimum, Φ_{min1} (deep energy "well" located close to the collector surface), the primary maximum, Φ_{max1} (energy barrier to attachment and detachment) and the secondary minimum, Φ_{min2} (shallow energy "well" located some distance away from the collector surface). In environmental systems, both colloids and soils typically have a negatively charged surface and thus there is an energy barrier to deposition of colloid [83]. If repulsive interactions are present, it is regarded as "unfavorable" for colloid deposition [190]. Retention in Φ_{min1} at the collector surface is considered to be irreversible due to the huge energy barrier to overcome, while retention on secondary minima is reversible under constant chemical conditions [188].

The actual adhesion energy variation as a function of separation distance between the interacting surfaces has been widely calculated by the classic DLVO theory [163,188]. However, the applicable condition of the theory is that both the colloidal particle surfaces and the collector should be chemically inert. Van Oss [191] extended DLVO theory (XDLVO) by accounting for the interactions of Lewis acid-base (Φ_{AB}), which are essential for describing the interfacial interactions of polar media (electron acceptor/electron donor interactions). It has been reported that the XDLVO theory might be a promising approach to explain the experimental results of bacteria deposition because it combines both DLVO theory and the thermodynamic approach [192]. The XDLVO theory considers retarded van der Waals interaction energy Φ_{VDW} [189], electrostatic double layer interaction energy Φ_{EL} [193] and Lewis acid/base interaction energy Φ_{AB}, for a particle (1), and a flat plate sediment grain or air bubble (2) in the water medium (3). These interaction energies can be calculated as follows:

$$\Phi_{tot}(\mathrm{h}) = \Phi_{VDW}(\mathrm{h}) + \Phi_{EL}(\mathrm{h}) + \Phi_{AB}(\mathrm{h}) \quad (12)$$

The Φ_{VDW}, Φ_{EL} and Φ_{AB} can be evaluated as follows:

$$\Phi_{VDW} = -\frac{\mathrm{A}_{132}\mathrm{a}_p}{6\mathrm{h}}\left[1 - \frac{5.32\mathrm{h}}{\lambda}\ln\left(1+\frac{\lambda}{5.32\mathrm{h}}\right)\right] \quad (13)$$

$$\mathrm{A}_{132} = 24\pi\mathrm{h}_0^2(\sqrt{\gamma_1^{LW}} - \sqrt{\gamma_3^{LW}})(\sqrt{\gamma_2^{LW}} - \sqrt{\gamma_3^{LW}}) \quad (14)$$

$$\Phi_{EL} = \pi\varepsilon_r\varepsilon_0\mathrm{a}_p(\Psi_{01}^2 + \Psi_{02}^2)\left[\frac{2\Psi_{01}\Psi_{02}}{(\Psi_{01}^2+\Psi_{02}^2)}\ln\left(\frac{1+\exp(-\kappa\mathrm{h})}{1-\exp(-\kappa\mathrm{h})}\right) + \ln(1-\exp(-2\kappa\mathrm{h}))\right] \quad (15)$$

$$\Phi_{AB} = 2\pi\mathrm{a}_p\lambda_{AB}\Delta\mathrm{G}_{h0}^{AB}\exp\left(\frac{\mathrm{h}_0-\mathrm{h}}{\lambda_{AB}}\right) \quad (16)$$

$$\Delta\mathrm{G}_{h0}^{AB} = 2[\sqrt{\gamma_3^+}(\sqrt{\gamma_1^-}+\sqrt{\gamma_2^-}-\sqrt{\gamma_3^-}) + \sqrt{\gamma_3^-}(\sqrt{\gamma_1^+}+\sqrt{\gamma_2^+}-\sqrt{\gamma_3^+}) - \sqrt{\gamma_1^-\gamma_2^+} - \sqrt{\gamma_1^+\gamma_2^-}] \quad (17)$$

where, h is the surface to surface distance (m); h_0 is the distance of closest approach (m) and equals to 0.157 nm at which Born repulsion is observed [194], λ_w is the characteristic wavelength (m), assumed to be 42.5 nm [195]; a_p is the radius of the bacterial cells (m); ε_r is the relative dielectric permittivity of water; ε_0 is the rela-

tive dielectric permittivity of vacuum; λ_{AB} is the decay length of water (m), taken as 0.2 nm; A_{132} (J) is the combined Hamaker constant for surfaces 1 and 2, which represents bacteria and porous media/air bubble, respectively, suspended in medium 3 (water); Ψ_{01} and Ψ_{02} are the surface potentials of bacteria and the porous media or air bubble (V), respectively, which can be evaluated as follows:

$$\Psi_0 = \xi\left(1+\frac{z}{r_i}\right)\exp(\kappa z) \tag{18}$$

where, ξ is the zeta potential at the shear plane (V); z is the distance from bacteria or porous media surface to the shear plane (m), taken to be 5 Å; r_i is the radius of bacteria or porous media (m); κ is the Debye-Huckel parameter.

The classic DLVO and XDLVO predictions for bacteria deposition have been previously studied by many researchers. The interaction energies for varied membrane-colloid combinations have been investigated, and it was observed that the XDLVO model predicts considerably different short-range interaction energies (separation distance is smaller than 10 nm) as compared to the classic DLVO model, especially for hydrophilic membrane-colloid combination [196]. Another study determined bacterial adhesion on various substrate surfaces and concluded that XDLVO theory can be more accurate in predicting bacterial adhesion than DLVO approach for a hydrophobic substratum surface [197].

The calculation of interaction energies by classic DLVO and XDLVO theory has also been done to describe bacterial adhesion in unsaturated porous media. In this case, it was observed that the Φ_{VDW} is attractive towards both the air and the grain, and the Φ_{AB} is attractive towards AWI and repulsive towards the grain [198].

2. Hydrophobic Interaction

The classical DLVO theory cannot describe hydrophobic interaction [199], owing to the thermodynamically unfavorable interactions of hydrophobic substances with water molecules [200]. Yoon et al. [187] proposed an alternative model based on empirical measurements to calculate hydrophobic interactions. On the basis of respective contact angles, hydrophobic interaction between two surfaces can be calculated [71,187].

The hydrophobic interaction between a colloid and a flat surface can be represented by the following expression:

$$\Phi_{hyd} = \int \frac{K_{123} a_p}{h^2} = -\frac{K_{123} a_p}{h} \tag{19}$$

where, a_p is the radius of colloid; K_{123} is the hydrophobic force constant which can be predicted by the empirical expression as follows [71,187]:

$$\log K_{123} = a\left(\frac{\cos\theta_1 + \cos\theta_2}{2}\right) + b \tag{20}$$

where, θ_1 is the contact angle on a colloid surface; θ_2 is the contact angle on a second surface (solid-water interface or air-water interface). Here, θ_2 at the air surface is taken as 180° [71]. The terms a and b are system-specific constants, where a=−5 and b=−20, were used for a system of air interface [71] and a=−6 and b=−22 were used for a system of solid surfaces [74].

Bradford and Torkzaban [27] reported that when the ionic strength of suspension was 10 mmol/L, the particles with contact angle smaller than 30° had a positive interaction energy near AWI. This indicated that particles would not be attached to air phase. However, Chen [198] calculated the interactions of van der Waals and Lewis acid-base, and observed that in the de-ionized water, the sum of all energies was negative at the biocolloid-AWI. Therefore, it was argued that the attachment of AWI had occurred. It can be concluded from these observations that the significance of hydrophobic interaction for hydrophilic colloids attachment to air remains unresolved [201].

3. Steric Interaction

Polymers have been employed to prevent the aggregation of colloids to control their stability in environmental systems [31], which is termed as steric stabilization. It has been reported that polymeric macromolecules and surfactants can be adsorbed on the suspended particles in solution, which can form layers with a thickness of 10-20 nm [31]. The adsorbed polymers may rearrange their positions and orientations because they are thermally mobile and can extend out from the surface into solution. Interactions between two layers can occur when the separation distance between the polymer coated surfaces is less than twice the adsorbed layer thickness. Steric interactions caused by the adsorbed chains and chain elements protruding from the adsorbed layer can be repulsive or attractive. The physical basis of steric interaction is the combination of osmotic effect and the volume restriction effect [31]. The osmotic effect is observed when the two surfaces with adsorbed polymers approach each other at a relatively high concentration, while volume restriction effect can occur when the possible configurations between the two surfaces with adsorbed polymers decrease [31].

According to de Gennes [202], two forces could contribute to the steric interactions between the two surfaces (Fig. 6): a) The elastic restoring forces which tend to thin out the brush, and b) The osmotic pressure inside each brush. The repulsive steric force per unit area (P) between the two parallel surfaces has been characterized by the following equation by de Gennes:

$$P = \frac{kT}{s_0^3}\left[\left(\frac{2l_0}{h}\right)^{9/4} - \left(\frac{h}{2l_0}\right)^{3/4}\right] \quad \text{For } h < 2l_0 \tag{21}$$

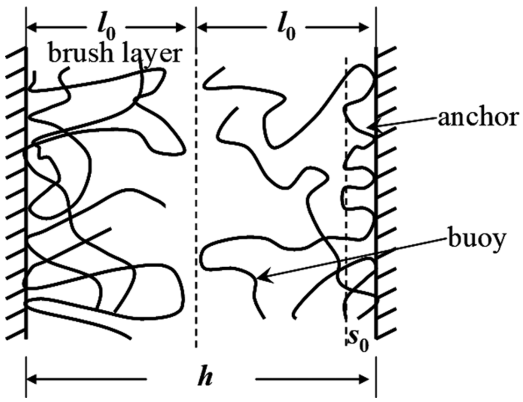

Fig. 6. Illustration of two parallel surfaces coated by macromolecules. The "anchor" precipitates against the wall while the "buoy" protrudes toward the solution (adapted from de Gennes [202]).

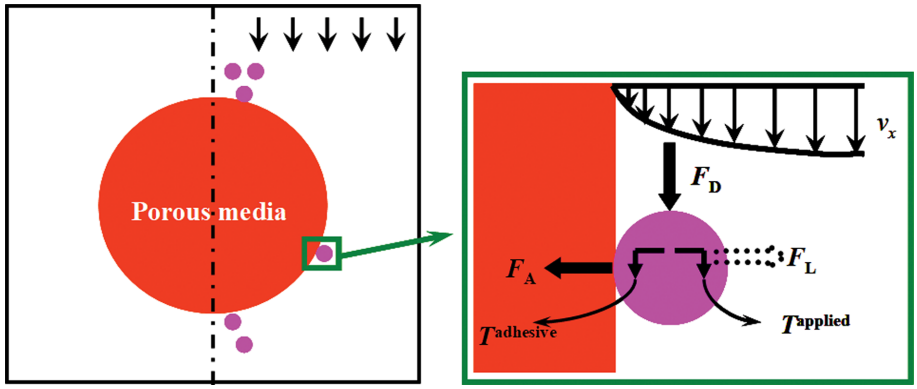

Fig. 7. A schematic representation of the hydrodynamic forces and torques that act on colloids attached on the porous media (adapted from Torkzaban et al. [214]).

where, h is the separation distance between both surfaces; l_0 is the brush layer thickness; and s_0 is the mean distance between anchoring sites. The values of l_0 and s_0 were taken as 30 nm and 2.2 nm, respectively [177,203]. The first and second term in the bracket represents the osmotic and the elastic term, respectively.

If one plate is bare and the other one has the brush, h will be substituted with 2h and the pressure will be divided by 2 [204]:

$$P=\frac{1}{2}\frac{kT}{s_0^3}\left[\left(\frac{l_0}{h}\right)^{9/4}-\left(\frac{h}{l_0}\right)^{3/4}\right] \quad \text{For } h<l_0 \tag{22}$$

One can get the expression of steric force by using the integration of Derjaguin's approximation for a plate-sphere system [203,205]:

$$\begin{aligned} F_{steric}(x)&=2\pi a_p\frac{1}{2}\frac{kT}{s_0^3}\int_h^{l_0}\left[\left(\frac{l_0}{x}\right)^{9/4}-\left(\frac{x}{l_0}\right)^{3/4}\right]dx \\ &=\frac{4l_0}{35}\pi a_p\frac{kT}{s_0^3}\left[5\left(\frac{h}{l_0}\right)^{7/4}+7\left(\frac{l_0}{h}\right)^{5/4}-12\right] \end{aligned} \tag{23}$$

The integration of F_{steric} gives the steric interaction energy (Φ_{steric}) using the following equation [203]:

$$\begin{aligned} \Phi_{steric}&=\int_h^{l_0}F(x)dx \\ &=\frac{4}{385}\pi a_p\frac{kT}{s_0^3}\left[-20h^3\left(\frac{h}{l_0}\right)^{3/4}+308l_0^3\left(\frac{h}{l_0}\right)^{3/4}-420hl_0^2+132h^2l_0\right] \end{aligned} \tag{24}$$

Pedersen and Bergstrom [206] studied the steric forces between a sphere-plate surface coated by zirconia that was immersed into the poly(acrylic acid) solution, and observed that the steric interactions predominated at an ionic strength of 0.01 mol/L when compared with the electrostatic contribution. The steric interactions between colloids (bacterial cells) and porous media were studied by a research group and it was reported that the cell surface polymers can interact directly with the surface of porous media to produce a steric repulsion [177]. However, for different microbial strains, the thickness of the macromolecular layer coated on the cell surface was different, which is an important parameter to govern the steric forces [177]. Therefore, the quantification of these characteristics for different microbial strains is needed to better understand the interactions of microbes of interest with their surrounding environments [207,208].

4. Hydrodynamic and Resisting Torques

Hydrodynamic conditions of the system may moderate the magnitude of DLVO, hydrophobic, steric and capillary forces. The effect of hydrodynamic conditions is more prominent for physicochemical attachment under unfavorable conditions [209,210]. The balance of hydrodynamic forces and torques on the colloids in a moving fluid particle, results in the detachment of colloids adhering to the porous medium surfaces [209,211].

The torque on the colloid adhering to a flat surface includes: (a) A drag force (F_D) which acts tangentially to the surface; (b) An adhesive force (F_A) that operates normal to the surface of porous media; and (c) A lift force (F_L), resulting due to the unsteady nature of viscous sub layer in the turbulent boundary layer [212], which operates normal to the surface (Fig. 7). The F_A binds the colloid to porous medium surface, while the other two forces (F_D and F_L) attempt to mobilize the colloid [212]. In most of the cases, the flow of water is laminar, and F_L is negligible compared to the opposing F_A which is thus omitted from the balance of the torques [213].

If the net F_A overcomes the hydrodynamic forces and the applied torques acting on colloids near to an interface, colloid attachment is observed [27]. The Derjaguin and Langbein approximations were used to obtain the adhesive force (F_A), the value of which was estimated as Φ_{min2}/h_s. Here, Φ_{min2} is the secondary minimum interaction energy (Nm), and h_s is the separation distance between solid surface and colloids (m). The resisting or adhesive torque ($T^{adhesive}$, Nm) for colloids attached in the DLVO secondary minimum is estimated as follows [210]:

$$T^{adhesive}=a_0F_A \tag{25}$$

where, F_A is DLVO force of colloid adhesion in the secondary minimum (N), and a_0 is the radius of the colloid-surface contact area [215]. The corresponding contact radius a_0 (m) can be estimated as follows [83]:

$$a_0=\left(\frac{4a_pF_A}{K_i}\right)^{1/3} \tag{26}$$

where, a_p is the colloid radius (m) and K_i is the constant of elastic interaction (N/m^2). The value of $K_i=4.014\times10^9$ N/m^2, estimated for glass beads and colloids by Bergendahl and Grasso [216].

Hydrodynamic forces can also act on colloids near to SWI or

AWI based on the water flow [27]. When the flow of water is laminar, F_L is negligible [217] and F_D (along the surface causing the colloid removal [212]) is significant and it can be calculated as follows [218]:

$$F_D = 10.205\pi\mu_w a_p^2\left(\frac{\partial v}{\partial r}\right) \quad (27)$$

where, a_p is the radius of colloid (m); μ_w is the viscosity of water (Pa·s); $\partial v/\partial r$ is the velocity shear rate acting on attached colloids (1/s); r is the radial direction from the surface of porous media (m); and v is the vector of pore scale velocity (m/s).

The applied hydrodynamic torque ($T^{applied}$) acting on the colloid is determined as [218]:

$$T^{applied} = 1.4a_p F_D = 14.287\pi\mu_w a_p^3\left(\frac{\partial v}{\partial r}\right) \quad (28)$$

The pore geometry in the porous media can be simplified by considering it as a bundle of capillary tubes with different sizes (Fig. S10). Thereafter, in a given capillary tube, the velocity shear rate can be deduced from Poiseuille's Law as follows [210]:

$$\frac{\partial v}{\partial r} = \frac{\Delta P}{2\mu_w L_{ct}}(R_{ct} - a_p) \quad (29)$$

where, R_{ct} is the capillary tube radius (m); ΔP is the pressure difference across the capillary tube (N/m^2); L_{ct} is the length of capillary tube (m); and $\Delta P/L_{ct}$ is the pressure gradient (N/m^3). From Eq. (29), the shear rate is proportional to the pressure gradient and radius of the capillary tube. For a given Darcy velocity and conductivity in a porous media, $\Delta P/L_{ct}$ can be determined by Darcy's Law as follows:

$$\frac{\Delta P}{L_{ct}} = \frac{q\mu_w}{k} \quad (30)$$

where, q is Darcy velocity (m/s), and k represents the intrinsic permeability of porous media (m^2).

A colloid that collides with the surface of porous media may not always succeed in attachment and may detach from the interface [27]. The balance between $T^{applied}$ and $T^{adhesive}$ determines if the colloids can remain immobilized on the interface. According to Bradford et al., colloid attachment can occur if the $T^{applied} < T^{adhesive}$ [210].

Various studies have examined the influence of hydrodynamics acting near the surfaces of porous media on the attachment of colloids. It was observed that when the $T^{applied}$ arising from hydrodynamic drag was one or more order of magnitude lower than the $T^{adhesive}$, the $T^{applied}$ was not enough to drive re-entrainment of colloid [83]. Torkzaban et al. [214] reported that if the $T^{adhesive}$ is larger than the $T^{applied}$, attachment can occur. Similar results were also reported by Bradford et al [210].

5. Capillary Forces

Capillary forces result from the capillary bridges of liquid-in-gas or gas-in-liquid, which bring about interactions between particle and wall of collectors [219]. Detailed information on the capillary forces is provided by Gao et al. [220] and Syngouna and Chrysikopoulos [184]. Briefly, the capillary force, F_c ($kg·m/s^2$), acting on a colloid trapped in a thin water film developed around the porous

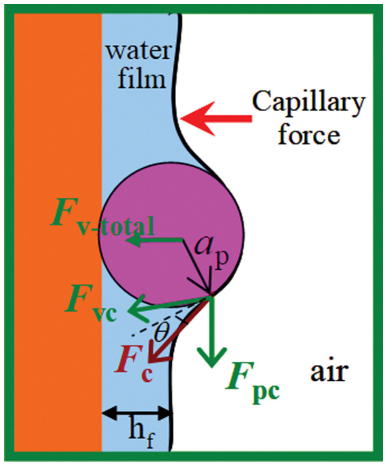

Fig. 8. Schematic representation of capillary forces (F_c) acting on bacteria trapped in a thin water film with thickness h_f (adapted from Syngouna and Chrysikopoulos [184]).

grain, includes two forces: a force F_{pc}, parallel to the porous media surface and a vertical force F_{vc}, perpendicular to the porous media surface (Fig. 8).

Consequently, the total force $F_{v\text{-}tot}$ with which the spherical bacteria with radius a_p (m), trapped within a water film with height h_f (m), is held against the surface of porous media can be represented as follows [184,220]:

$$F_{v\text{-}tot} = \sigma_{aw} 2\pi\sqrt{a_p^2 - (h_f - a_p)^2}\cos\left[\theta + \frac{\pi}{2} - \cos^{-1}\left(\frac{h_f - a_p}{a_p}\right)\right] \quad (31)$$

The interaction of the capillary force over its path in the direction of the force through the water film gives the capillary potential energy, Φ_c (J), for a colloid that protrudes out a distance, d_f, of either AWS interface or a film [184,220]. The capillary potential energy can be represented as follows:

$$\begin{aligned}\Phi_c &= \int_{z=r_p(1-\cos\theta)}^{z=d_f} F_{v\text{-}tot}\,dz \\ &= \int_{z=r_p 1-\cos\theta}^{z=d_f} \sigma_{aw} 2\pi\sqrt{a_p^2 - (a_p - z)^2}\cos\left[\theta + \frac{\pi}{2} - \cos^{-1}\left(\frac{a_p - z}{a_p}\right)\right]dz\end{aligned} \quad (32)$$

where, σ_{aw} is the air-water surface tension (0.0718 N/m at 25 °C), and θ is the contact angle between water and colloid (°).

Wan and Tokunaga [73] developed an equation to predict the thickness of a water film, w_f (m):

$$w_f = \left(\frac{\varepsilon_r \varepsilon_0}{2}\right)^{1/2}\left(\frac{\pi kT}{ve}\right)\left(\frac{4\sigma_{aw}}{d_c} - \psi\right)^{-1/2} \quad (33)$$

where, ε_r and ε_0 are the relative dielectric permittivity of water (78.55 at 25 °C), and the relative dielectric permittivity of a vacuum, respectively; k is Boltzmann's constant; T is the absolute temperature (K); v is the ionic charge; e is the electron charge; σ_{aw} is the air-water surface tension; d_m is the median grain diameter (m); and ψ is the matric potential that represents the saturation-dependent component of the chemical potential of water (Pa) [73]. Under critical saturation conditions (when pendular rings become discontinuous) and under close packing (rhombohedral) of uniform spherical grains with diameter d_m, the critical matric poten-

tial is given by the following equation [73,221]:

$$\psi_c = -\frac{9.068\,\sigma_{aw}}{d_m} \quad (34)$$

If the water film thickness is smaller than the colloid diameters, film straining can occur [221,222].

It has been reported that the capillary forces can contribute to bacterial retention [220]. These forces act within the water films or at AWS interfaces. Capillary forces are also observed to result in colloid straining at air-water meniscus-solid (AW_mS) interface [223]. Gao et al. [220] reported that the capillary energy potential for film straining of colloids was several orders higher than the DLVO energy potential. Similar results were also reported by Syngouna and Chrysikopoulos [184].

RESEARCH METHODS OF BIOCOLLOID TRANSPORT AND DEPOSITION IN POROUS MEDIA

1. Field-scale Experiments

Investigations on biocolloid transport through subsurface media are important to assess the risk of water contamination, to estimate the setback distance of receiving water and disposal field, and to select a proper site for water reclamation [224]. Many field studies have been carried out to determine the potential of pathogenic organism transport from their sources to drinking water supply wells. In the last few decades, local scale controlled injection and recovery tests have been performed to investigate the bacterial transport mechanisms at the field-scale [225-230].

Bales et al. [230] carried out the experiments which mainly focused on the effect of pH on the remobilization and attenuation of a virus, and observed bacterial breakthrough at a distance of 11 m. Sinton et al. [228] investigated the transport velocities of three microbial species through 16.8 m deep vadose zone at a sewage treatment plant, and observed them to be between 15.7 m/h and 39.2 m/h. It was also observed that the microbial mass could still reach the groundwater through macropores, which was beneath the effluent irrigation schemes [228]. Weaver et al. [229] injected bacteria and virus into coastal sand aquifers and observed the breakthrough at three monitoring wells at 5 m, 2.5 m and 1 m distances from the injection well. Large amounts of MS2 phage and *E. coli* J6-2 were observed to be removed due to the low levels of contamination, which can increase their attachment to aquifer. Anders and Chrysikopoulos [231] performed a field-scale experiment of the viruses (MS2 and PRD1) fate and transport during artificial recharge with recycled water, and observed virus concentrations were fitted using a mathematical model accounting for virus sorption, virus inactivation and time-dependent source concentration. The corresponding time-dependent collision efficiencies for both bacteriophage asymptotically reached similar values at the various sampling locations. Masciopinto et al. [232] investigated the fate and transport of pathogens in a fractured aquifer in the Salento area, Italy. They suggested that for the municipal wastewater injected into the Nardò aquifer the required most conservative setback distance for drinking wells should be over 8,000 m. Field-scale transport tests can provide valuable information about biocolloid transport through soil in nature, but it is difficult to obtain a high degree of control over the experimental conditions. Moreover, these tests are not easy to conduct and repeat compared to the laboratory column-scale experiments.

2. Laboratory Experiments at Macroscopic Column Scale

Laboratory column experiments are traditional methods to study colloid behavior in porous media. A colloid suspension is injected via peristaltic pump into columns packed with porous media, and the colloids collected from the effluent are analyzed with a UV/visible spectrophotometer, or any other method, to produce breakthrough curves (BTCs) of the colloids. The BTCs provide useful information to characterize the transport of colloids into the column. After the completion of transport experiment, the packed column can be disassembled and the porous media can be carefully excavated and recovered into small vials. Colloids retained in the porous media are eluted using excess solution and their concentration is measured by different analytic methods. Column dissection provides information regarding the colloid retention profiles. Moreover, by fitting a transport model to the observed breakthrough curve and retention profile data points, some mechanistic interpretations of the colloid-grain interactions can be made. A summary of the representative studies on the colloid transport and deposition using laboratory column experiments is presented in Table S1. Thus, both laboratory column studies and field experiments can provide useful information on the mechanisms involved in the transport and deposition of colloids at macroscopic scale, but they cannot provide direct observations at pore scale, particularly about the colloid interactions with different interfaces.

3. Laboratory Experiments at Microscopic Pore Scale

Based on the direct observation of colloid interactions with the interface, microscopic pore scale experiment can complement the breakthrough measurements by investigating colloid interactions with water, as well as with air and solid interfaces. They can also investigate colloid locations relative to medium grains or various interfaces at pore scale. Pore scale experiments can be employed to determine the relative importance of colloid transport and retention mechanisms, and to verify the presumed mechanisms. A micromodel system consists of a pump used to inject a colloid suspension into the medium, a porous network, and an imaging system, which commonly consists of a camera or confocal microscope coupled with a device for capturing video images.

Sirivithayapakorn and Keller [233] investigated the attachment of colloids with different sizes on AWI using epifluorescence microscopy and observed that when the distance between colloids and AWI was small enough, the collision caused the final attachment of colloids onto the interface. Although these studies have shown preferential partitioning of colloids at AWI, most recent studies reported SWI to play a key role in some cases such as ionic strength, chemically heterogeneous porous media, *etc.* [234]. Saiers and Lenhart [234] developed a relationship between water saturation degree and the capacity of colloid retention at SWI/AWI, and reported that colloid deposition on SWI rapidly increased as the ionic strength increased. When the ionic strength increases over a critical value (0.1-0.2 mol/L), SWI deposition becomes a dominant mechanism compared to AWI affinity. Bradford et al. [55] examined the deposition behavior of bacteria through a fine sand in a specially designed micro-model and observed the bacteria to

be deposited in small pores, grain junctions or pore constrictions because of straining. Another study used a pore-scale visualization method to study colloid retention in sandy porous media and observed the colloids to be retained near the AWS [75]. The *Cryptosporidium parvum* oocyst retention mechanism in the quartz sand was also investigated using micro-model methods [235]. It was concluded that the majority of oocysts were retained in low velocity regions. The colloid straining at pore space constrictions was also observed, along with a few colloids deposited in the center of the sand grains, away from the grain-grain contacts, suggesting physicochemical deposition was limited by strong repulsive forces between sand and colloids [52].

CONCLUSIONS AND FUTURE PERSPECTIVES

This review summarizes the current understanding of biocolloid transport and deposition mechanisms in porous media and the main influencing chemicals, as well as the influencing physicochemical, physical and biological factors, to provide a better insight into the environmental behavior of biocolloids. Biocolloid transport and deposition depend on many factors, including porous media characteristics, solution chemistry, hydrodynamic conditions as well as biology of the cells. However, studies that have investigated such factors are not always in agreement, possibly due to the many variables involved. Generally, the effect of biological properties, such as motility, hydrophobicity of cell surface, and cell zeta potential on transport and retention through homogeneous or fine-sand media has been widely studied. However, the respective studies using physically heterogeneous or aggregated porous media are less documented. Also, studies performed under saturated conditions are more common than those under unsaturated conditions. Developing an understanding of the interaction between biocolloids and SWI/AWI/SWA interfaces in a heterogeneous or aggregated media is necessary to understand the complex process in groundwater ecosystems. In the existing literature, many experimental and theoretical studies have investigated various interaction potential energies. The determination of both DLVO and non-DLVO interactions, such as hydrodynamic forces, steric interactions, hydrophobic interactions and capillary potential energies, shows that biocolloid deposition in saturated and unsaturated porous media is influenced by both kinds of interactions. However, under unfavorable conditions for chemical attachment, the capillary forces may be several orders of magnitude stronger than the other forces under unsaturated conditions, and might be the dominant forces responsible for bacterial deposition via film straining. Therefore, to have a good understanding of biocolloid interactions with porous media, especially under unfavorable conditions for physicochemical attachment and under unsaturated flow conditions, there is a need for a global theory including DLVO and non-DLVO interactions.

Field-scale transport experiments do provide valuable information on biocolloid transport through the soil in nature, but it is not easy due to the complexity of physical and/or chemical conditions and their dynamic evolution, compared to the well-controlled conditions in laboratory column-scale experiments. Laboratory column and field experiments only show a combined effect of all relevant mechanisms, but cannot give direct information about colloid interactions with SWI, AWI and AWS. Microscopic pore scale experiments can complement the breakthrough measurements. Although microscopic pore scale study can improve our understanding of the movement of microbial pathogens in the geologic and engineered systems, developing quantitative and qualitative relationships for micro-scale attachment and detachment rate coefficients is needed and might be the target for future research.

To be noted is that the results in the published literature are obtained from studies performed with only one bacterial strain or virus. Thus, the conclusions obtained should not be generalized and might not be applicable to more complex and field conditions. Moreover, additional studies to investigate processes involved in different biocolloid interactions on sorption sites and their influence in natural communities on the migration dynamics in groundwater systems, need to have a more realistic understanding of biocolloid transport and deposition mechanisms.

ACKNOWLEDGEMENTS

The authors would like to acknowledge the financial support provided by research funds from Université de Technologie de Compiègne and the financial support of National Natural Science Foundation of China (No. 41807120; No. U1904171), the Fundamental Research Funds for the Henan Provincial Colleges and Universities in Henan University of Technology (No. 2018QNJH01), Doctor Foundation of Henan University of Technology (No. 2018BS003), Science Foundation of Henan University of Technology (No. 2017RCJH09) and Science and Technology Foundation of Henan Province (No. 212102310026; No. 202102310208; No. 182102410092) and the Young Backbone Teachers Training Program Foundation of Henan University of Technology (No. 2021GGJS-063).

LIST OF ABBREVIATIONS AND SYMBOLS

Abbreviations

AWI : air-water interface
AWS : air-water-solid interface
AWmS : air-water meniscus-solid
CFT : colloid filtration theory
DLVO : Derjaguin-Landau-Verwey-Overbeek
EPS : extracellular polymeric substances
GO NPs : graphene oxide nanoparticles
LPS : lipopolysaccharides
SWI : solid-water interface
XDLVO : extended Derjaguin-Landau-Verwey-Overbeek

Symbols

A_{aw} : air-water interfacial area per unit volume [L^2L^{-3}]
A : hamaker constant [$M{\cdot}L^2{\cdot}T^{-2}$]
a : system-specific hydrophobic constant [-]
a_0 : colloid radius [L]
A_{132} : combined hamaker constant for two surfaces [$M{\cdot}L^2{\cdot}T^{-2}$]
a_p : radius of colloid/bacteria [L]
B_a : growth/death of the microbes at air-water interface [$NL^{-3}T^{-1}$]
B_s : growth/death of the microbes on the solid phase [$NL^{-3}T^{-1}$]

B_w : growth/death of the microbes in the water phase [$NL^{-3}T^{-1}$]
b : system-specific hydrophobic constant [-]
b_w : empirical parameters [T]
C : concentration in the liquid phase [$M \cdot L^{-3}$]
C_{max} : maximum concentration associated with the upper limit of population growth [$M \cdot L^{-3}$].
D : dispersion coefficient [$L^2 \cdot T^{-1}$]
d_{10} : grain diameter at which 10% of porous media by mass are smaller [L]
d_{60} : grain diameter at which 60% of porous media by mass are smaller [L]
d_b : microbe diameter [L]
d_f : distance for a bacteria protruding out of a film [L]
d_m : median grain diameter [L]
d_p : median pore diameter of porous media [L]
e : electron charge, 1.602×10^{-19} C
F_A : adhesive force [$M \cdot L \cdot T^{-2}$]
F_c : capillary force [$M \cdot L \cdot T^{-2}$]
F_D : drag force [$M \cdot L \cdot T^{-2}$]
F_L : lift force [$M \cdot L \cdot T^{-2}$]
F_{pc} : parallel capillary force [$M \cdot L \cdot T^{-2}$]
F_{steric} : steric force [$M \cdot L \cdot T^{-2}$]
F_{vc} : vertical/perpendicular capillary force [$M \cdot L \cdot T^{-2}$]
$F_{v\text{-}tot}$: total vertical capillary force [$M \cdot L \cdot T^{-2}$]
G : free energy of interaction [$M \cdot T^{-2}$]
h : distance of separation [L]
$H(z-z_0)$: heaviside function
h_0 : distance of closest approach [L]
h_f : thickness of the bacteria trapped in a thin water film [L]
h_s : separation distance between colloid and solid surface [L]
I : ionic strength [$M \cdot L^{-3}$]
k : Boltzmann's constant, 1.3805×10^{-23} J/K
k : intrinsic permeability of a porous medium [L^2]
K_{123} : hydrophobic force constant [-]
k_{aaw} : attachment coefficient to the AWI [T^{-1}]
k_{daw} : detachment coefficient to the AWI [T^{-1}]
k_{asw} : attachment coefficient to the SWI [T^{-1}]
k_{dsw} : detachment coefficient to the SWI [T^{-1}]
K_i : elastic interaction constant, 4.014×10^9 N/m^2
k_{str} : straining coefficient [T^{-1}]
l_0 : thickness of the brush layer [L]
L_{ct} : capillary tube length [L]
m : empirical coefficient [-]
M : total amount of the contaminant in the soil [M]
N_A : avogadro constant, 6.022×10^{23}
N_c : counts of biocolloid [-]
P : pressure [$M \cdot L^{-1} \cdot T^{-2}$]
P : steric force per unit area [$M \cdot L^{-1} \cdot T^{-2}$]
P_d : probability of pendular ring discontinuity [-]
q : darcy velocity [$L \cdot T^{-1}$]
q_c : volumetric water flux density for colloids [LT^{-1}]
r : radial direction from the solid surface [L]
R_{ct} : radius of a given capillary tube [L]
r_i : radius of bacteria or porous media [-]
s : solid phase concentration on the porous medium [$N_c \cdot M^{-1}$]
s_0 : distance between anchoring sites [L]
T : absolute temperature [K]
t : time [T]
$T^{adhesive}$: resisting or adhesive torque [$M \cdot L^2 \cdot T^{-2}$]
$T^{applied}$: applied hydrodynamic torque [$M \cdot L^2 \cdot T^{-2}$]
v : ionic charge [-]
w_f : water film [L]
X : coefficient of death/inactivation [T^{-1}]
z : vertical coordinate [L]
z_0 : coordinate of the location where the straining process starts [L]

Greek Symbols

α_s : total sticking efficiency [-]
Γ : microbe concentration retained on the AWI [NL^{-2}]
γ^+ : electron-acceptor parameter [$M \cdot T^{-2}$]
γ^- : electron-donor parameter [$M \cdot T^{-2}$]
γ^{LW} : Lifshitz-van der Waals component of surface tension [$M \cdot T^{-2}$]
ε_0 : permittivity under vacuum, 8.854×10^{-12} C/(Vm)
ε_r : relative dielectric permittivity of water, 78.55 for water at 25 °C
ζ : empirical parameters [T^{-1}]
η_0 : single collector contact efficiency [-]
θ : volumetric moisture content [$L^3 \cdot L^{-3}$]
θ_1 : contact angle on a colloid surface
θ_2 : contact angle on SWI or AWI
θ_c : volumetric water content accessible to microbes [$L^3 \cdot L^{-3}$]
κ : Debye-Huckel parameter
Λ : microbe growth coefficient [$NL^{-3}T^{-1}$]
Λ_0 : growth rate in the absence of competition [T^{-1}]
λ_{AB} : decay length of water [L]
λ_w : characteristic wavelength [L]
μ_w : water viscosity [$M \cdot L^{-1} \cdot T^{-1}$]
ν_e : valence of the electrolyte
ξ : zeta potential [V]
ξ' : empirical coefficient
ρ_b : bulk density [$M \cdot L^{-3}$]
σ_{aw} : air-water surface tension, 0.0718 N/m at 25 °C
Φ_{AB} : lewis acid/base interaction energy [$M \cdot L^2 \cdot T^{-2}$]
Φ_c : capillary potential energy [$M \cdot L^2 \cdot T^{-2}$]
Φ_{EL} : electrostatic double layer interactions [$M \cdot L^2 \cdot T^{-2}$]
Φ_{min1} : primary maximum [$M \cdot L^2 \cdot T^{-2}$]
Φ_{min2} : secondary minimum [$M \cdot L^2 \cdot T^{-2}$]
Φ_{steric} : steric interaction energy [$M \cdot L^2 \cdot T^{-2}$]
Φ_{tot} : total interaction energy [$M \cdot L^2 \cdot T^{-2}$]
Φ_{VDW} : van der Waals forces [$M \cdot L^2 \cdot T^{-2}$]
ψ : matric potential [$M \cdot L^{-1} \cdot T^{-2}$]
ψ_c : critical matric potential [$M \cdot L^{-1} \cdot T^{-2}$]
Ψ_0 : surface potential [V]
Ψ_{01} : surface potential of bacteria [V]
Ψ_{02} : surface potential of porous media/air bubble [V]
ψ_{aw} : dimensionless function on the AWI [-]
ψ_{sw} : dimensionless function on the SWI [-]
ψ_{str} : depth-dependent deposition coefficient [-]
Ω : empirical factor controlling the shape of the retention profile [-]
ω_i : empirical parameters [T^{-1}]
ω_{str} : film straining rate coefficient [T^{-1}]

SUPPORTING INFORMATION

Additional information as noted in the text. This information is available via the Internet at http://www.springer.com/chemistry/journal/11814.

REFERENCES

1. J. F. McCarthy and L. D. McKay, *Vadose Zone J.*, **3**, 326 (2004).
2. J. E. Saiers and J. N. Ryan, *Water Resour. Res.*, **42**, W12S01 (2006).
3. J. F. McCarthy and J. M. Zachara, *Environ. Sci. Technol.*, **23**, 496 (1989).
4. C. V. Chrysikopoulos and Y. Sim, *J. Hydrol.*, **185**, 199 (1996).
5. B. H. Keswick and C. P. Gerba, *Environ. Sci. Technol.*, **14**, 1290 (1980).
6. T. R. Ginn, B. D. Wood, K. E. Nelson, T. D. Scheibe, E. M. Murphy and T. P. Clement, *Adv. Water Resour.*, **25**, 1017 (2002).
7. K. A. Reynolds, *Water Condit. Purif.*, **56**, 28 (2004).
8. T. K. Sen, D. Das, K. C. Khilar and G. K. Suraishkumar, *Colloids Surf. A: Physicochem. Eng. Asp.*, **260**, 53 (2005).
9. A. Unc and M. J. Goss, *Appl. Soil Ecol.*, **25**, 1 (2004).
10. C. Hagedorn, D. T. Hansen and G. H. Simonson, *J. Environ. Qual.*, **7**, 54 (1978).
11. C. Ray, T. W. Soong, Y. Q. Lian and G. S. Roadcap, *J. Hydrol.*, **266**, 235 (2002).
12. W. J. Weiss, E. J. Bouwer, R. Aboytes, M. W. LeChevallier, C. R. O'Melia, B. T. Le and K. J. Schwab, *Water Res.*, **39**, 1990 (2005).
13. I. M. Banat, *Bioresour. Technol.*, **51**, 1 (1995).
14. N. Tufenkji, J. N. Ryan and M. Elimelech, *Environ. Sci. Technol.*, **36**, 422a (2002).
15. J. F. Schijven and S. M. Hassanizadeh, *Crit. Rev. Env. Sci. Tec.*, **30**, 49 (2000).
16. J. W. A. Foppen and J. F. Schijven, *Water Res.*, **40**, 401 (2006).
17. N. Tufenkji, *Adv. Water Resour.*, **30**, 1455 (2007).
18. H. B. Zhang, N. A. Nordin and M. S. Olson, *J. Contam. Hydrol.*, **150**, 54 (2013).
19. A. Safadoust, A. A. Mahboubi, M. R. Mosaddeghi, B. Gharabaghi, A. Unc, P. Voroney and A. Heydari, *J. Hydrol.*, **430-431**, 80 (2012).
20. H. J. Bai, N. Cochet, A. Pauss and E. Lamy, *Colloids Surf. B: Biointerfaces*, **139**, 148 (2016).
21. Z. Dong, H. Y. Yang, D. Wu, J. R. Ni, H. Kim and M. P. Tong, *Colloids Surf. B: Biointerfaces*, **123**, 995 (2014).
22. H. J. Bai, N. Cochet, A. Pauss and E. Lamy, *Colloids Surf. B: Biointerfaces*, **150**, 41 (2017).
23. D. Wu, L. He, R. N. Sun, M. P. Tong and H. Kim, *Water Res.*, **121**, 1 (2017).
24. Y. Zhao, D. Qu, R. Zhou, X. Yang, W. Kong and H. Ren, *Environ. Sci. Pollut. Res.*, **25**, 26539 (2018).
25. K. S. Balkhair, *Water Res.*, **110**, 313 (2017).
26. A. A. Keller and M. Auset, *Adv. Water Resour.*, **30**, 1392 (2007).
27. S. A. Bradford and S. Torkzaban, *Vadose Zone J.*, **7**, 667 (2008).
28. E. Engström, R. Thunvik, R. Kulabako and B. Balfors, *Crit. Rev. Env. Sci. Tec.*, **45**, 1 (2015).
29. N. J. Jarvis, *Eur. J. Soil Sci.*, **58**, 523 (2007).
30. S. A. Bradford, V. L. Morales, W. Zhang, R. W. Harvey, A. I. Packman, A. Mohanram and C. Welty, *Crit. Rev. Env. Sci. Tec.*, **43**, 775 (2013).
31. D. Grasso, K. Subramaniam, M. Butkus, K. Strevett and J. Bergendahl, *Rev. Environ. Sci. Biotechnol.*, **1**, 17 (2002).
32. T. Kristian Stevik, A. Kari, G. Ausland and J. Fredrik Hanssen, *Water Res.*, **38**, 1355 (2004).
33. J. M. Köhne, S. Köhne and J. Šimůnek, *J. Contam. Hydrol.*, **104**, 4 (2009).
34. T. K. Stevik, K. Aa, G. Ausland and J. F. Hanssen, *Water Res.*, **38**, 1355 (2004).
35. L. M. McDowell-Boyer, J. R. Hunt and N. Sitar, *Water Resour. Res.*, **22**, 1901 (1986).
36. R. W. Buddemeier and J. R. Hunt, *Appl. Geochem.*, **3**, 535 (1988).
37. W. K. Ng, V. Jegatheesan and S.-H. Lee, *Korean J. Chem. Eng.*, **23**, 333 (2006).
38. T. Baumann and C. J. Werth, *Vadose Zone J.*, **3**, 434 (2004).
39. M. Auset and A. A. Keller, *Water Resour. Res.*, **40**, W03503 (2004).
40. K. Yao, M. T. Habibian and C.R. O'Melia, *Environ. Sci. Technol.*, **5**, 105 (1971).
41. R. Rajagopalan and C. Tien, *AIChE J.*, **22**, 523 (1976).
42. R. Rajagopalan, C. Tien, R. Pfeffer and G. Tardos, *AIChE J.*, **28**, 871 (1982).
43. J. N. Ryan and M. Elimelech, *Colloids Surf. A: Physicochem. Eng. Aspects*, **107**, 1 (1996).
44. S. A. Bradford, J. Šimůnek, M. Bettahar, M. T. van Genuchten and S. R. Yates, *Environ. Sci. Technol.*, **37**, 2242 (2003).
45. R. Kretzschmar and T. Schäfer, *Elements*, **1**, 205 (2005).
46. M. S. Willis and I. Tosun, *Chem. Eng. Sci.*, **35**, 2427 (1980).
47. S. A. Bradford, S. R. Yates, M. Bettahar and J. Šimůnek, *Water Resour. Res.*, **38**, 1327 (2002).
48. J. P. Herzig, D. M. Leclerc and P. Le Goff, *Ind. Eng. Chem.*, **62**, 8 (1970).
49. G. Gargiulo, S. A. Bradford, J. Šimůnek, P. Ustohal, H. Vereecken and E. Klumpp, *Vadose Zone J.*, **7**, 406 (2008).
50. S. A. Bradford and M. Bettahar, *J. Contam. Hydrol.*, **82**, 99 (2006).
51. S. A. Bradford, Y. F. Tadassa and Y. Pachepsky, *J. Environ. Qual.*, **35**, 749 (2006).
52. S. P. Xu, B. Gao and J. E. Saiers, *Water Resour. Res.*, **42**, W12S16 (2006).
53. N. Tufenkji, J. A. Redman and M. Elimelech, *Environ. Sci. Technol.*, **37**, 616 (2003).
54. S. A. Bradford and M. Bettahar, *J. Environ. Qual.*, **34**, 469 (2005).
55. S. A. Bradford, J. Šimůnek and S. L. Walker, *Water Resour. Res.*, **42**, W12S12 (2006).
56. W. P. Johnson, E. Pazmino and H. Ma, *Water Res.*, **44**, 1158 (2010).
57. S. Torkzaban, H. N. Kim, J. Šimůnek and S. A. Bradford, *Environ. Sci. Technol.*, **44**, 1662 (2010).
58. S. A. Bradford, V. L. Morales, W. Zhang, R. W. Harvey, A. I. Packman, A. Mohanram and C. Welty, *Crit. Rev. Env. Sci. Tec.*, **43**, 775 (2013).
59. A. Parvan, S. Jafari, M. Rahnama, S. Norouzi-Apourvari and A. Raoof, *Adv. Water Resou.*, **151**, 103888 (2021).
60. A. Parvan, S. Jafari, M. Rahnama, S. Norouzi apourvari and A. Raoof, *Adv. Water Resou.*, **138**, 103530 (2020).
61. M. Samari-Kermani, S. Jafari, M. Rahnama and A. Raoof, *Colloid Interface Sci.*, **42**, 100389 (2021).
62. C. H. Bolster, S. L. Walker and K. L. Cook, *J. Environ. Qual.*, **35**, 1018 (2006).

63. V. I. Syngouna, C. V. Chrysikopoulos, P. Kokkinos, M. A. Tselepi and A. Vantarakis, *Sci. Total Environ.*, **598**, 160 (2017).
64. Q. Li, J. K. Yang, W. Fan, D. D. Zhou, X. Y. Wang, L. L. Zhang, M. X. Huo and J. C. Crittenden, *Colloids Surf. B: Biointerfaces*, **162**, 35 (2018).
65. Z. G. Ning, R. Li, K. T. Lian, P. Liao, H. H. Liao and C. X. Liu, *Chemosphere*, **233**, 57 (2019).
66. N. Sepehrnia, A. A. Mahboubi, M. R. Mosaddeghi, A. A. Safari Sinejani and G. Khodakaramian, *Geoderma*, **217-218**, 83 (2014).
67. A. Safadoust, A. A. Mahboubi, M. R. Mosaddeghi, B. Gharabaghi, A. Unc, P. Voroney and A. Heydari, *J. Hydrol.*, **430-431**, 80 (2012).
68. G. X. Chen and S. L. Walker, *Environ. Sci. Technol.*, **46**, 8782 (2012).
69. C. V. Chrysikopoulos and A. F. Aravantinou, *J. Environ. Chem. Eng.*, **2**, 796 (2014).
70. J. M. Wan and J. L. Wilson, *Water Resour. Res.*, **30**, 11 (1994).
71. A. Schäfer, H. Harms and A. J. B. Zehnder, *Environ. Sci. Technol.*, **32**, 3704 (1998).
72. J. E. Saiers and J. J. Lenhart, *Water Resour. Res.*, **39**, 1019 (2003).
73. J. M. Wan and T. K. Tokunaga, *Environ. Sci. Technol.*, **31**, 2413 (1997).
74. J. T. Crist, Y. Zevi, J. F. McCarthy, J. A. Throop and T. S. Steenhuis, *Vadose Zone J.*, **4**, 184 (2005).
75. J. T. Crist, J. F. McCarthy, Y. Zevi, P. Baveye, J. A. Throop and T. S. Steenhuis, *Vadose Zone J.*, **3**, 444 (2004).
76. Y. Zevi, A. Dathe, J. F. McCarthy, B. K. Richards and T. S. Steenhuis, *Environ. Sci. Technol.*, **39**, 7055 (2005).
77. Y. Zevi, A. Dathe, B. Gao, B. K. Richards and T. S. Steenhuis, *Water Resour. Res.*, **42**, W12S03 (2006).
78. J. J. Lenhart and J. E. Saiers, *Environ. Sci. Technol.*, **36**, 769 (2002).
79. J. Šimůnek, N. J. Jarvis, M. T. van Genuchten and A. Gärdenäs, *J. Hydrol.*, **272**, 14 (2003).
80. J. Šimůnek, M. T. van Genuchten and M. Šejna, *Vadose Zone J.*, **7**, 587 (2008).
81. N. Tufenkji and M. Elimelech, *Environ. Sci. Technol.*, **38**, 529 (2004).
82. J. A. Redman, S. B. Grant, T. M. Olson and M. K. Estes, *Environ. Sci. Technol.*, **35**, 1798 (2001).
83. X. Q. Li, P. F. Zhang, C. L. Lin and W. P. Johnson, *Environ. Sci. Technol.*, **39**, 4012 (2005).
84. P. R. Johnson and M. Elimelech, *Langmuir*, **11**, 801 (1995).
85. C. H. Bolster, A. L. Mills, G. M. Hornberger and J. S. Herman, *J. Contam. Hydrol.*, **50**, 287 (2001).
86. J. F. Schijven and J. Šimůnek, *J. Contam. Hydrol.*, **55**, 113 (2002).
87. G. Gargiulo, S. A. Bradford, J. Šimůnek, P. Ustohal, H. Vereecken and E. Klumpp, *J. Contam. Hydrol.*, **92**, 255 (2007).
88. M. Peleg and M. B. Cole, *Crit. Rev. Food Sci. Nutr.*, **38**, 353 (1998).
89. Y. Sim and C. V. Chrysikopoulos, *Transport Porous Med.*, **30**, 87 (1998).
90. V. E. Katzourakis and C. V. Chrysikopoulos, *Ground Water*, **55**, 156 (2017).
91. V. E. Katzourakis and C. V. Chrysikopoulos, *J. Contam. Hydrol.*, **181**, 102 (2015).
92. Y. Sim and C. V. Chrysikopoulos, *Water Resour. Res.*, **31**, 1429 (1995).
93. Y. Sim and C. V. Chrysikopoulos, *Water Resour. Res.*, **32**, 2607 (1996).
94. V. E. Katzourakis and C. V. Chrysikopoulos, *Water Resour. Res.*, **54**, 3841 (2018).
95. N. Kresic, *Hydrogeology and groudwater modeling*, CRC Press, New York (2006).
96. S. Bhattacharjee, J. N. Ryan and M. ELImelech, *J. Contam. Hydrol.*, **57**, 161 (2002).
97. J. E. Saiers and J. N. Ryan, *Geophys. Res. Lett.*, **32**, L21406 (2005).
98. G. Gargiulo, S. A. Bradford, J. Šimůnek, P. Ustohal, H. Vereecken and E. Klumpp, *J. Contam. Hydrol.*, **92**, 255 (2007).
99. N. Tufenkji, G. F. Miller, J. N. Ryan, R. W. Harvey and M. Elimelech, *Environ. Sci. Technol.*, **38**, 5932 (2004).
100. G. Chen and K. A. Strevett, *Environ. Microbiol.*, **3**, 237 (2001).
101. J. W. A. Foppen, A. Mporokoso and J. F. Schijven, *J. Contam. Hydrol.*, **76**, 191 (2005).
102. C. Shani, N. Weisbrod and A. Yakirevich, *Colloids Surf. A: Physicochem. Eng. Asp.*, **316**, 142 (2008).
103. A. Benamar, N. D. Ahfir, H. Q. Wang and A. Alem, *C. R. Geoscience*, **339**, 674 (2007).
104. Y. Y. Sun, B. Gao, S. A. Bradford, L. Wu, H. Chen, X. Q. Shi and J. C. Wu, *Water Res.*, **68**, 24 (2015).
105. B. B. Ding, C. L. Li, M. Zhang, F. Ji and X. Q. Dong, *Chem. Eng. Sci.*, **127**, 40 (2015).
106. J. W. A. Foppen and J. F. Schijven, *Water Res.*, **39**, 3082 (2005).
107. D. E. Fontes, A. L. Mills, G. M. Hornberger and J. S. Herman, *Appl. Environ. Microbiol.*, **57**, 2473 (1991).
108. B. Gharabaghi, A. Safadoust, A. A. Mahboubi, M. R. Mosaddeghi, A. Unc, B. Ahrens and G. Sayyad, *J. Hydrol.*, **522**, 418 (2015).
109. F. K. Leij, S. A. Bradford, *J. Contam. Hydrol.*, **150**, 65 (2013).
110. R. W. Harvey, N. E. Kinner, D. MacDonald, D. W. Metge and A. Bunn, *Water Resour. Res.*, **29**, 2713 (1993).
111. L. P. Pang, M. McLeod, J. Aislabie, J. Šimůnek, M. Close and R. Hector, *Vadose Zone J.*, **7**, 97 (2008).
112. S. Jiang, L. P. Pang, G. D. Buchan, J. Šimůnek, M. J. Noonan and M. E. Close, *Water Res.*, **44**, 1050 (2010).
113. A. Safadoust, A. A. Mahboubi, M. R. Mosaddeghi, B. Gharabaghi, P. Voroney, A. Unc and G. Khodakaramian, *J. Environ. Manage.*, **107**, 147 (2012).
114. S. J. Pirson, *Bull. Amer. Assoc. Petrol. Geol.*, **37**, 232 (1953).
115. A. Coppola, M. Kutílek and E. O. Frind, *J. Contam. Hydrol.*, **104**, 1 (2009).
116. F. P. Brennan, G. Kramers, J. Grant, V. O'Flaherty, N. M. Holden and K. Richards, *Soil Sci. Soc. Am. J.*, **76**, 663 (2012).
117. S. B. Kim, S. J. Park, C. G. Lee, N. C. Choi and D. J. Kim, *Colloids Surf. B: Biointerfaces*, **63**, 236 (2008).
118. H. Dong, T. C. Onstott, M. F. DeFlaun, M. E. Fuller, T. D. Scheibe, S. H. Streger, R. K. Rothmel and B. J. Mailloux, *Environ. Sci. Technol.*, **36**, 891 (2002).
119. E. Cullen, D. M. O'Carroll, E. K. Yanful and B. Sleep, *Adv. Water Resour.*, **33**, 361 (2010).
120. M. R. Soltanian and R. W. Ritzi, *Water Resour. Res.*, **50**, 9766 (2014).
121. E. M. Murphy, T. R. Ginn, A. Chilakapati, C. T. Resch, J. L. Phillips, T. W. Wietsma and C. M. Spadoni, *Water Resour. Res.*, **33**, 1087 (1997).
122. M. R. Soltanian, R. W. Ritzi, Z. Dai and C. C. Huang, *Chemosphere*, **122**, 235 (2015).
123. S. A. Bradford, S. Sasidharan, H. Kim and G. Hwang, *Front. Env. Sci.*, **6**, 1 (2018).
124. C. Y. Shen, S. A. Bradford, T. T. Li, B. G. Li and Y. F. Huang, *J.*

Nanopart. Res., **20**, 165 (2018).
125. N. Tufenkji and M. Elimelech, *Langmuir*, **21**, 841 (2005).
126. J. P. Loveland, S. Bhattacharjee, J. N. Ryan and M. Elimelech, *J. Contam. Hydrol.*, **65**, 161 (2003).
127. P. Babakhani, J. Bridge, R. Doong and T. Phenrat, *Water Resour. Res.*, **53**, 4564 (2017).
128. P. Babakhani, J. Bridge, R. Doong and T. Phenrat, *Adv. Colloid Int. Sci.*, **246**, 75 (2017).
129. P. Babakhani, F. Fagerlund, A. Shamsai, G. V. Lowry and T. Phenrat, *Environ. Sci. Pollut. Res.*, **25**, 7180 (2018).
130. B. Huang, A. J. Miao, L. Xiao and L. Y. Yang, *Environ. Sci.: Nano*, **4**, 1840 (2017).
131. D. Mahmoudi, M. Rezaei, J. Ashjari, E. Salehghamari, F. Jazaei and P. Babakhani, *Sci. Total Environ.*, **729**, 138804 (2020).
132. H. N. Kim and S. L. Walker, *Colloids Surf. B: Biointerfaces*, **71**, 160 (2009).
133. H. N. Kim, S. A. Bradford and S. L. Walker, *Environ. Sci. Technol.*, **43**, 4340 (2009).
134. J. J. Johanson, L. Feriancikova, A. Banerjee, D. A. Saffarini, L. X. Wang, J. Li, T. J. Grundl and S. P. Xu, *Colloids Surf. B: Biointerfaces*, **123**, 439 (2014).
135. Y. S. Wang, S. A. Bradford and J. Šimůnek, *Water Resour. Res.*, **49**, 2424 (2013).
136. Y. S. Wang, S. A. Bradford and J. Šimůnek, *Vadose Zone J.*, **13**, vzj2013.07.0120 (2013).
137. H. X. Zhang, A. C. Ulrich and Y. Liu, *Colloids Surf. B: Biointerfaces*, **130**, 110 (2015).
138. B. Z. Haznedaroglu, H. N. Kim, S. A. Bradford and S. L. Walker, *Environ. Sci. Technol.*, **43**, 1838 (2009).
139. D. Janjaroen, Y. Y. Liu, M. S. Kuhlenschmidt, T. B. Kuhlenschmidt and T. H. Nguyen, *Environ. Sci. Technol.*, **44**, 4519 (2010).
140. G. Sadeghi, J. F. Schijven, T. Behrends, S. M. Hassanizadeh, J. Gerritse and P. J. Kleingeld, *Ground Water*, **49**, 12 (2011).
141. D. G. Jewett, T. A. Hilbert, B. E. Logan, R. G. Arnold and R. C. Bales, *Water Res.*, **29**, 1673 (1995).
142. T. A. Stenström, *Appl. Environ. Microbiol.*, **55**, 142 (1989).
143. Y. Sim and C. V. Chrysikopoulos, *Colloid Surface A*, **155**, 189 (1999).
144. Y. Sim and C. V. Chrysikopoulos, *Water Resour. Res.*, **36**, 173 (2000).
145. R. Anders and C. V. Chrysikopoulos, *Transp. Porous Med.*, **76**, 121 (2009).
146. S. Torkzaban, S. M. Hassanizadeh, J. F. Schijven and H. H. J. L. van der Berg, *Water Resour. Res.*, **42**, W12S14 (2006).
147. A. Schäfer, P. Ustohal, H. Harms, F. Stauffer, T. Dracos and J. B. A. Zehnder, *J. Contam. Hydrol.*, **33**, 149 (1998).
148. M. P. Tong and W. P. Johnson, *Environ. Sci. Technol.*, **40**, 7725 (2006).
149. A. A. Keller, S. Sirivithayapakorn and C. V. Chrysikopoulos, *Water Resour. Res.*, **40**, 2003WR002676 (2004).
150. M. Samari-Kermani, S. Jafari, M. Rahnama and A. Raoof, *Adv. Water Resour.*, **144**, 103694 (2020).
151. W. P. Johnson, X. Q. Li and S. Assemi, *Adv. Water Resour.*, **30**, 1432 (2007).
152. M. Elimelech, J. Y. Chen and Z. A. Kuznar, *Langmuir*, **19**, 6594 (2003).
153. P. Kokkinos, V. I. Syngouna, M. A. Tselepi, M. Bellou, C. V. Chrysikopoulos and A. Vantarakis, *Food Environ. Virol.*, **7**, 122 (2015).
154. J. T. Gannon, V. B. Manilal and M. Alexander, *Appl. Environ. Microbiol.*, **57**, 190 (1991).
155. M. Y. Corapcioglu and A. Haridas, *J. Hydrol.*, **72**, 149 (1984).
156. T. H. Weiss, A. L. Mills, G. M. Hornberger and J. S. Herman, *Environ. Sci. Technol.*, **29**, 1737 (1995).
157. H. Gadekar and J. Karia, *Gujarat Med. J.*, **65**, 27 (2010).
158. S. A. Burt, R. van der Zee, A. P. Koets, A. M. de Graaff, F. van Knapen, W. Gaastra, H. P. Haagsman and E. J. A. Veldhuizen, *Appl. Environ. Microbiol.*, **73**, 4484 (2007).
159. H. C. Berg, *Nature*, **249**, 77 (1974).
160. M. C. M. van Loosdrecht, J. Lyklema, W. Norde and A. J. B. Zehnder, *Microbial Ecology*, **17**, 1 (1989).
161. M. W. Becker, S. A. Collins, D. W. Metge, R. W. Harvey and A. M. Shapiro, *J. Contam. Hydrol.*, **69**, 195 (2004).
162. G. Gargiulo, S. A. Bradford, J. Šimůnek, P. Ustohal, H. Vereecken and E. Klumpp, *Environ. Sci. Technol.*, **41**, 1265 (2007).
163. S. L. Walker, J. A. Redman and M. Elimelech, *Environ. Sci. Technol.*, **39**, 6405 (2005).
164. C. Tanford, *Science*, **200**, 1012 (1978).
165. W. Mamo, *Rev. Sci. Tech.*, **8**, 163 (1989).
166. A. H. Hogt, J. Dankert and J. Feijen, *FEMS Microbiol. Letters*, **18**, 211 (1983).
167. M. Rosenberg, H. Judes and E. Weiss, *Infect. Immun.*, **42**, 831 (1983).
168. G. I. Geertsema, H. C. van der Mei and H. J. Busscher, *J. Microbiol. Method*, **18**, 61 (1993).
169. H. van der Mei, R. Bos and H. J. Busscher, *Colloids Surf. B: Biointerfaces*, **11**, 213 (1998).
170. M. C. M. van Loosdrecht, J. Lyklema, W. Norde, G. Schraa and A. J. B. Zehnder, *Appl. Environ. Microbiol.*, **53**, 1893 (1987).
171. D. R. McCaulou, R. C. Bales and J. F. McCarthy, *J. Contam. Hydrol.*, **15**, 1 (1994).
172. H. Chang, A. Ikam, F. Kosari, G. Vasmatzis, A. Bhunia and R. Bashir, *J. Vac. Sci. Technol. B.*, **20**, 2058 (2002).
173. G. Harkes, H. van der Mei, P. Rouxhet, J. Cankert, H. Busscher and J. Feijen, *Cell Biophysics*, **20**, 17 (1992).
174. A. Jacobs, F. Lafolie, J. M. Herry and M. Debroux, *Colloids Surf. B: Biointerfaces*, **59**, 35 (2007).
175. T. J. Beveridge, *Int. Rev. Cytol.*, **72**, 229 (1981).
176. T. J. Beveridge and S. F. Koval, *Appl. Environ. Microbiol.*, **42**, 325 (1981).
177. G. X. Chen and S. L. Walker, *Environ. Sci. Technol.*, **46**, 8782 (2012).
178. S. L. Walker, J. A. Redman and M. Elimelech, *Langmuir*, **20**, 7736 (2004).
179. A. Omoike and J. Chorover, *Biomacromolecules*, **5**, 1219 (2004).
180. X. J. Dai and R. M. Hozalski, *Water Res.*, **36**, 3523 (2002).
181. M. P. Georgopoulou, V. I. Syngouna and C. V. Chrysikopoulos, *Colloids Surf. B: Biointerfaces*, **189**, 110841 (2020).
182. V. I. Syngouna and C. V. Chrysikopoulos, *Sci. Total Environ.*, **545-546**, 210 (2016).
183. V. I. Syngouna and C. V. Chrysikopoulos, *Colloid Surface A*, **416**, 56 (2013).
184. V. I. Syngouna and C. V. Chrysikopoulos, *J. Colloid Interface Sci.*, **440**, 140 (2015).

185. V. E. Katzourakis and C. V. Chrysikopoulos, *Adv. Water Resour.*, **68**, 62 (2014).
186. M. I. Bellou, V. I. Syngouna, M. A. Tselepi, P. A. Kokkinos, S. C. Paparrodopoulos, A. Vantarakis and C. V. Chrysikopoulos, *Sci. Total Environ.*, **517**, 86 (2015).
187. R. H. Yoon, D. H. Flinn and Y. I. Rabinovich, *J. Colloid Interface Sci.*, **185**, 363 (1997).
188. J. A. Redman, S. L. Walker and M. Elimelech, *Environ. Sci. Technol.*, **38**, 1777 (2004).
189. J. Gregory, *J. Colloid Interface Sci.*, **83**, 138 (1981).
190. C. Y. Shen, B. G. Li, Y. F. Huang and Y. Jin, *Environ. Sci. Technol.*, **41**, 6976 (2007).
191. C. J. van Oss, *Colloids Surf. A: Physicochem. Eng. Asp.*, **78**, 1 (1993).
192. J. Azeredo, J. Visser and R. Oliveira, *Colloids Surf. B: Biointerfaces*, **14**, 141 (1999).
193. R. Hogg, T. W. Healy and D. W. Fuerstenau, *Trans. Faraday Soc.*, **62**, 1638 (1966).
194. E. Ruckenstein and D. C. Prieve, *AIChE J.*, **22**, 276 (1976).
195. L. Suresh and J. Walz, *J. Colloid Interface Sci.*, **183**, 199 (1996).
196. J. A. Brant and A. E. Childress, *Environ. Sci. Technol.*, **19**, 413 (2002).
197. J. M. Meinders, H. C. vanderMei and H. J. Busscher, *J. Colloid Interface Sci.*, **176**, 329 (1995).
198. G. Chen, *Colloids Surf. B: Biointerfaces*, **67**, 265 (2008).
199. S. W. Swanton, *Adv. Colloid Interface Sci.*, **54**, 129 (1995).
200. D. A. Wait and M. D. Sobsey, *Appl. Environ. Microbiol.*, **46**, 379 (1983).
201. V. Lazouskaya and Y. Jin, *Colloids Surf. A: Physicochem. Eng. Aspects*, **325**, 141 (2008).
202. P. G. de Gennes, *Adv. Colloid Interface Sci.*, **27**, 189 (1987).
203. L. X. Wang, S. P. Xu and J. Li, *Environ. Sci. Technol.*, **45**, 9566 (2011).
204. S. J. Oshea, M. E. Welland and T. Rayment, *Langmuir*, **9**, 1826 (1993).
205. H. J. Butt, B. Cappella and M. Kappl, *Surf. Sci. Rep.*, **59**, 1 (2005).
206. H. G. Pedersen and L. Bergstrom, *J. Amer. Chem. Soc.*, **82**, 1137 (1999).
207. E. S. Taylor and S. K. Lower, *Appl. Environ. Microbiol.*, **74**, 309 (2008).
208. L. S. Dorobantu, S. Bhattacharjee, J. M. Foght and M. R. Gray, *Langmuir*, **25**, 6968 (2009).
209. J. A. Bergendahl and D. Grasso, *Environ. Sci. Technol.*, **37**, 2317 (2003).
210. S. A. Bradford, S. Torkzaban and S. L. Walker, *Water Res.*, **41**, 3012 (2007).
211. M. A. Hubbe, *Colloids Surf.*, **16**, 249 (1985).
212. T. K. Sen and K. C. Khilar, *Adv. Colloid Interface Sci.*, **119**, 71 (2006).
213. S. K. Das, R. S. Schechter and M. M. Sharma, *J. Colloid Interface Sci.*, **164**, 63 (1994).
214. S. Torkzaban, S. A. Bradford and S. L. Walker, *Langmuir*, **23**, 9652 (2007).
215. K. L. Johnson, K. Kendall and A. D. Roberts, *Proc. R. Soc. London Ser. A*, **11**, 301 (1971).
216. J. Bergendahl and D. Grasso, *Chem. Eng. Sci.*, **55**, 1523 (2000).
217. M. Soltani and G. Ahmadi, *J. Adhes. Sci. Technol.*, **8**, 763 (1994).
218. A. J. Goldman, R. G. Cox and H. Brenner, *Chem. Eng. Sci.*, **22**, 653 (1967).
219. P. A. Kralchevsky and N. D. Denkov, *Curr. Opin. Colloid Interface Sci.*, **6**, 383 (2001).
220. B. Gao, T. S. Steenhuis, Y. Zevi, V. L. Morales, J. L. Nieber, B. K. Richards, J. F. McCarthy and J. Y. Parlange, *Water Resour. Res.*, **44**, W04504 (2008).
221. P. N. Mitropoulou, V. I. Syngouna and C. V. Chrysikopoulos, *Chem. Eng. J.*, **232**, 237 (2013).
222. S. Takahashi and A. R. Kovscek, *J. Petrol. Sci. Eng.*, **71**, 47 (2010).
223. Y. Zevi, A. Dathe, J. F. McCarthy, B. K. Richards and T. S. Steenhuis, *Environ. Sci. Technol.*, **39**, 7055 (2005).
224. L. P. Pang, *J. Environ. Qual.*, **38**, 1531 (2009).
225. R. C. Bales, S. M. Li, T. C. J. Yeh, M. E. Lenczewski and C. P. Gerba, *Water Resour. Res.*, **33**, 639 (1997).
226. J. F. Schijven, G. Medema, A. J. Vogelaar and S. M. Hassanizadeh, *J. Contam. Hydrol.*, **44**, 301 (2000).
227. W. W. Woessner, P. N. Ball, D. C. DeBorde and T. L. Troy, *Ground Water*, **39**, 886 (2001).
228. L. W. Sinton, R. R. Braithwaite, C. H. Hall, L. P. Pang, M. E. Close and M. J. Noonan, *Water Air Soil Pollut.*, **166**, 287 (2005).
229. L. Weaver, L. W. Sinton, L. P. Pang, R. Dann and M. Close, *Sci. Total Environ.*, **443**, 55 (2013).
230. R. C. Bales, S. M. Li, K. M. Maguire, M. T. Yahya, C. P. Gerba and R. W. Harvey, *Ground Water*, **33**, 653 (1995).
231. R. Anders and C. V. Chrysikopoulos, *Water Resour. Res.*, **41**, 2004WR003419 (2005).
232. C. Masciopinto, R. La Mantia and C. V. Chrysikopoulos, *Water Resour. Res.*, **44**, 2006WR005643 (2008).
233. S. Sirivithayapakorn and A. A. Keller, *Water Resour. Res.*, **39**, 1346 (2003).
234. J. E. Saiers and J. J. Lenhart, *Water Resour. Res.*, **39**, 1256 (2003).
235. H. N. Kim, S. L. Walker and S. A. Bradford, *Water Res.*, **44**, 1213 (2010).

Supporting Information

Biocolloid transport and deposition in porous media: A review

Hongjuan Bai*, Junhang Chen*,†, Yumu Hu*, Gang Wang*,†, Wenju Liu*,†, and Edvina Lamy**

*School of Chemistry and Chemical Engineering, Henan University of Technology, Zhengzhou 450001, P. R. China
**Sorbonne universités, Université de Technologie de Compiègne, UTC/ESCOM, EA 4297 TIMR,
Centre de recherche Royallieu - CS 60 319 - 60 203 Compiègne Cedex, France
(*Received 17 April 2021 • Revised 13 August 2021 • Accepted 26 August 2021*)

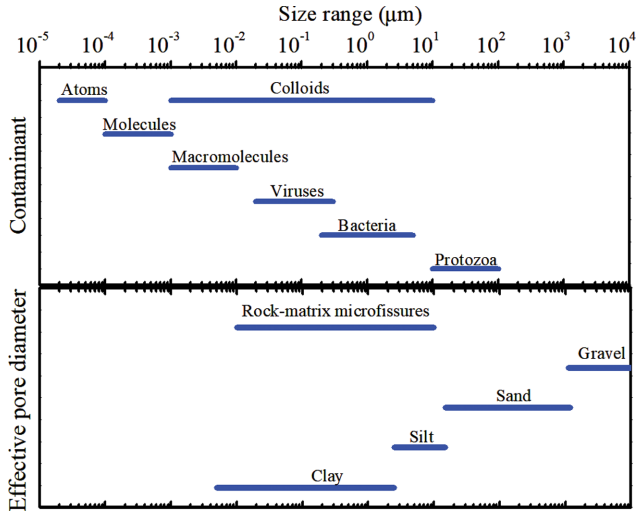

Fig. S1. Size ranges of microorganisms and colloids present in groundwater and effective pore diameters of various porous media (adapted from Chrysikopoulos and Sim [1]).

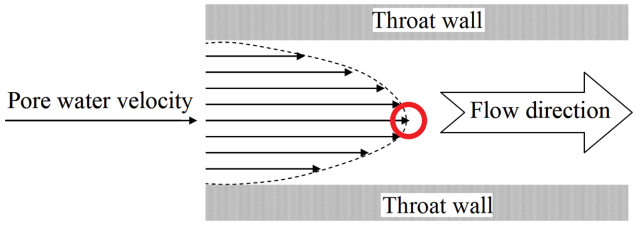

Fig. S2. Sketch of pore water velocity profile of colloid (red circle) in a pore throat (modified from Sirivithayapakorn and Keller [2]).

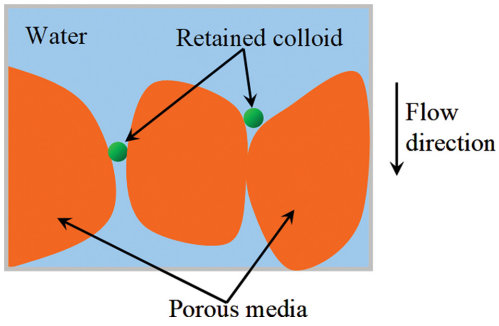

Fig. S3. Conceptual drawing of straining of colloid in the pore throat and grain-to-grain crevice of porous media.

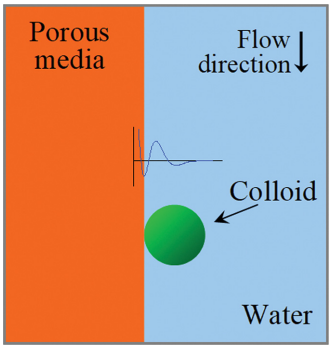

Fig. S4. Conceptual drawing of colloid attachment at a solid-water interface.

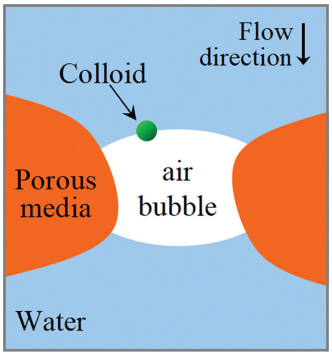

Fig. S5. Conceptual drawing of colloid attachment at the air-water interface.

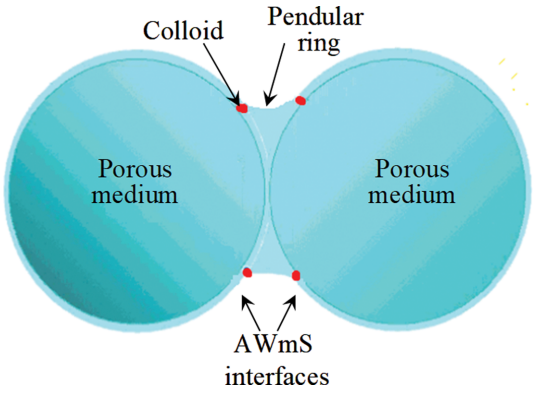

Fig. S6. Conceptual diagram of air-water meniscus-solid (AWmS) interfaces on two porous media, and colloids retained at the AWmS interfaces (modified from Zevi et al. [3]).

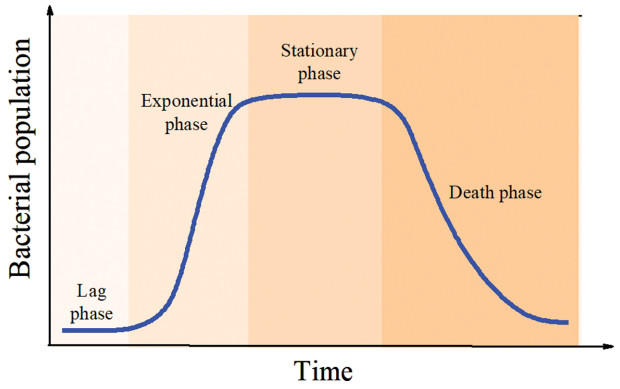

Fig. S7. Illustration of typical bacterial growth curve in a nutrient liquid batch culture.

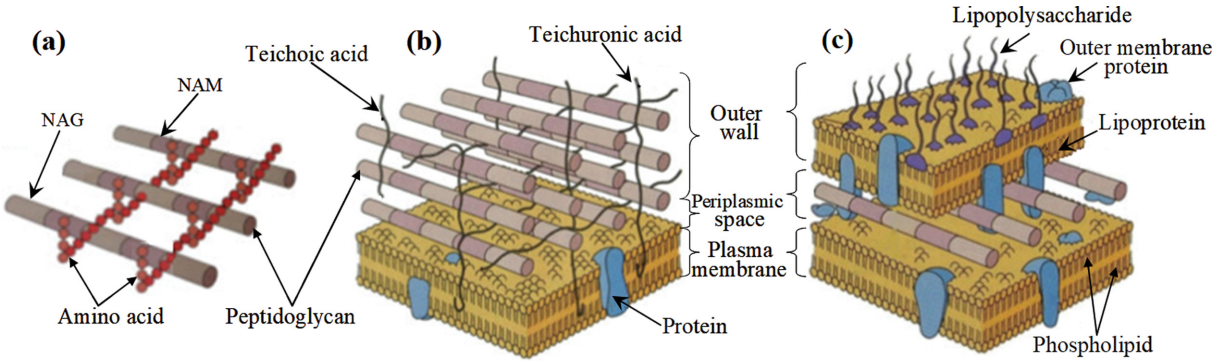

Fig. S8. Schematic illustration of the two types of bacteria cell wall. (a) Structure of peptidoglycan (NAG: *N*-acetylglucosamine acid and NAM: *N*-acetylmuramic acid), (b) cell wall of the gram-positive bacteria and (c) cell wall of the gram-negative bacteria (modified from Tortora et al. [4]).

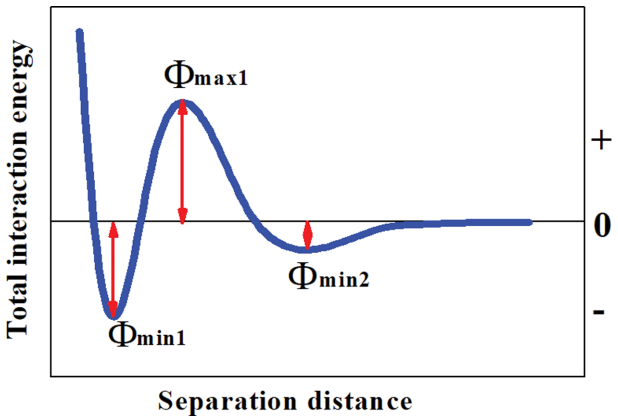

Fig. S9. Illustration of DLVO potential energy as a function of separation distance between colloid and collector (redrawn from [5]).

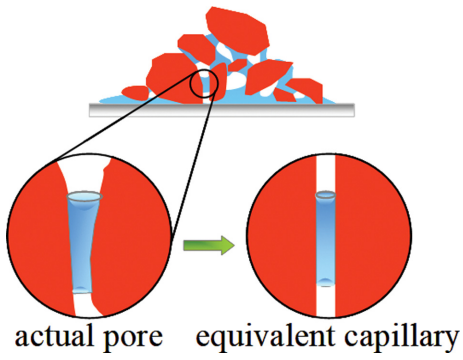

Fig. S10. Idealization of the soil pore space as cylindrical capillaries (adapted from Or and Wraith [6]).

Table S1. Representative studies investigating colloid transport and retention in porous media using laboratory column experiments

Colloid	Porous media	Factors explored	Reference
Klebsiella oxytoca and *Burkholderia cepacia*	Silica sand	Water velocity	[7]
Escherichia coli, MS2 and ΦX174	Quartz sand	Water velocity and grain size	[5]
Colloids and MS2	Sand	Water velocity and grain size	[8]
Bacteriophage PRD1	Quartz sand	pH and ionic strength	[9]
Escherichia coli ATCC 11105	Quartz sand	pH and coated sand content	[10]
Escherichia coli O157:H7	Quartz sand	Ionic strength and cell acclimation time	[11]
Escherichia coli	Field soil	Variable water chemistry	[12]
Rhodococcus rhodochrous	Silica sand	Grain size and bacteria surface protein	[13]
RNA coliphage, MS2, and *Salmonella typhimurium* phage	Monterey sand	Water content	[14]
Pseudomonas putida	Clays	Clay mineral structure	[15]
Escherichia coli, *Giardia lamblia cysts*	Agricultural soils	Organic matter and clay contents	[16]
Cryptosporidium parvum oocysts	Glass beads	Organic matter and biofilm	[17]
Escherichia coli NAR	clay/sandy loam soils	Soil structure	[18]
W31 and E3W7	quartz sand	Surface coatings and ionic strength	[19]
ML1, ML2, ML2m, and ML3	Glass bead	Cell characteristics and motility	[20]
Escherichia coli and *Campylobacter jejuni*	Quartz sand	Cell properties	[21]
Pseudomonas aeruginosa	Quartz surfaces	Motility	[22]
Escherichia coli K12	Quartz sands	Growth Phase	[23]
Escherichia coli NAR	clay/sandy loam soils	Temperature	[24]
Escherichia coli K12	Quartz sands	Cell starvation, pH and ionic strength	[25]
Escherichia coli HB101	Zeolite clays	Geological formation	[26]
Escherichia coli and *Bacteroides fragilis*	Quartz sands	Ionic strength	[27]
Dehalococcoides, *Geobacter*, and *Methanomethylovorans*	Glass beads	Ionic strength	[28]
Escherichia coli D21g	Ottawa sands	Ionic strength	[29]
Enterococcus faecalis and *Escherichia coli*	Quartz sand	Water content and Ionic strength	[30]

REFERENCES

1. C. V. Chrysikopoulos and Y. Sim, *J. Hydrol.*, **185**, 199 (1996).
2. S. Sirivithayapakorn and A. A. Keller, *Water Resour. Res.*, **39**, 2003WR002487 (2003).
3. Y. Zevi, A. Dathe, J. F. McCarthy, B. K. Richards and T. S. Steenhuis, *Environ. Sci. Technol.*, **39**, 7055 (2005).
4. G. J. Tortora, B. R. Funke and C. L. Case, *Introduction à la microbiologie*, Saint-Laurent, Québe (2003).
5. V. I. Syngouna and C. V. Chrysikopoulos, *J. Contam. Hydrol.*, **126**, 301 (2011).
6. D. Or and J. M. Wraith, *Soil Physics Companion*, **1**, 49 (2002).
7. M. J. Hendry, J. R. Lawrence and P. Maloszewski, *Ground Water*, **37**, 103 (1999).
8. A. A. Keller, S. Sirivithayapakorn and C. V. Chrysikopoulos, *Water Res. Resour.*, **40**, 2003WR002676 (2004).
9. G. Sadeghi, J. F. Schijven, T. Behrends, S. M. Hassanizadeh, J. Gerritse and P. J. Kleingeld, *Ground Water*, **49**, 12 (2011).
10. S. B. Kim, S. J. Park, C. G. Lee, N. C. Choi and D. J. Kim, *Colloids Surf. B: Biointerfaces*, **63**, 236 (2008).
11. F. D. Castro and N. Tufenkji, *Environ. Sci. Technol.*, **41**, 4332 (2007).
12. H. B. Zhang, N. A. Nordin and M. S. Olson, *J. Contam. Hydrol.*, **150**, 54 (2013).
13. G. Gargiulo, S. Bradford, J. Šimůnek, P. Ustohal, H. Vereecken and E. Klumpp, *J. Contam. Hydrol.*, **92**, 255 (2007).
14. R. Anders and C. V. Chrysikopoulos, *Transport Porous Med.*, **76**, 121 (2009).
15. I. A. Vasiliadou, D. Papoulis, C. V. Chrysikopoulos, D. Panagiotaras, E. Karakosta, M. Fardis and G. Papavassiliou, *Colloids Surf. B: Biointerfaces*, **84**, 354 (2011).
16. O. Landa-Cansigno, J. C. Durán-Álvarez and B. Jiménez-Cisneros, *J. Environ. Manage.*, **128**, 22 (2013).
17. X. Dai and R. M. Hozalski, *Water Res.*, **36**, 3523 (2002).
18. A. Safadoust, A. A. Mahboubi, M. R. Mosaddeghi, B. Gharabaghi, A. Unc, P. Voroney and A. Heydari, *J. Hydrol.*, **430-431**, 80 (2012).
19. C. H. Bolster, A. L. Mills, G. M. Hornberger and J. S. Herman, *J. Contam. Hydrol.*, **50**, 287 (2001).
20. M. W. Becker, S. A. Collins, D. W. Metge, R. W. Harvey and A. M. Shapiro, *J. Contam. Hydrol.*, **69**, 195 (2004).
21. C. H. Bolster, S. L. Walker and K. L. Cook, *J. Environ. Qual.*, **35**, 1018 (2006).
22. A. J. de Kerchove and M. Elimelech, *Environ. Sci. Technol.*, **42**, 4371 (2008).
23. S. L. Walker, J. A. Redman and M. Elimelech, *Environ. Sci. Technol.*, **39**, 6405 (2005).
24. B. Gharabaghi, A. Safadoust, A. A. Mahboubi, M. R. Mosaddeghi, A. Unc, B. Ahrens and G. Sayyad, *J. Hydrol.*, **522**, 418 (2015).
25. J. J. Walczak, L. X. Wang, S. L. Bardy, L. Feriancikova, J. Li and S. P. Xu, *Colloids Surf. B: Biointerfaces*, **90**, 129 (2012).

26. K. Vu, G. Yang, B. Y. Wang, K. Tawfiq and G. Chen, *Colloids Surf. B: Biointerfaces*, **125**, 45 (2015).
27. J. J. Johanson, L. Feriancikova, A. Banerjee, D. A. Saffarini, L. X. Wang, J. Li, T. J. Grundl and S. P. Xu, *Colloids Surf. B: Biointerfaces*, **123**, 439 (2014).
28. H. X. Zhang, A. C. Ulrich and Y. Liu, *Colloids Surf. B: Biointerfaces*, **130**, 110 (2015).
29. Y. S. Wang, S. A. Bradford and J. Šimůnek, *Vadose Zone J.*, **13**, vzj2013.07.0120 (2013).
30. G. X. Chen and S. L. Walker, *Environ. Sci. Technol.*, **46**, 8782 (2012).